ELSEVIER

^{13}C–^{18}O bonds in carbonate minerals: A new kind of paleothermometer

Prosenjit Ghosh [a,*], Jess Adkins [a], Hagit Affek [a], Brian Balta [a], Weifu Guo [a],
Edwin A. Schauble [b], Dan Schrag [c], John M. Eiler [a]

[a] *Division of Geological and Planetary Sciences, California Institute of Technology, Pasadena, CA 91125, USA*
[b] *Department of Earth and Space Sciences, University of California—Los Angeles, Los Angeles, CA 90095, USA*
[c] *Department of Earth and Planetary Sciences, Harvard University, Cambridge, MA 02138-2902, USA*

Abstract

The abundance of the doubly substituted CO_2 isotopologue, $^{13}C^{18}O^{16}O$, in CO_2 produced by phosphoric acid digestion of synthetic, inorganic calcite and natural, biogenic aragonite is proportional to the concentration of ^{13}C–^{18}O bonds in reactant carbonate, and the concentration of these bonds is a function of the temperature of carbonate growth. This proportionality can be described between 1 and 50 °C by the function: $\Delta_{47} = 0.0592 \cdot 10^6 \cdot T^{-2} - 0.02$, where Δ_{47} is the enrichment, in per mil, of $^{13}C^{18}O^{16}O$ in CO_2 relative to the amount expected for a stochastic (random) distribution of isotopes among all CO_2 isotopologues, and T is the temperature in Kelvin. This relationship can be used for a new kind of carbonate paleothermometry, where the temperature-dependent property of interest is the state of ordering of ^{13}C and ^{18}O in the carbonate lattice (i.e., bound together vs. separated into different CO_3^{2-} units), and not the bulk $\delta^{18}O$ or $\delta^{13}C$ values. Current analytical methods limit precision of this thermometer to ca. ± 2 °C, 1σ. A key feature of this thermometer is that it is thermodynamically based, like the traditional carbonate–water paleothermometer, and so is suitable for interpolation and even modest extrapolation, yet is rigorously independent of the $\delta^{18}O$ of water and $\delta^{13}C$ of DIC from which carbonate grew. Thus, this technique can be applied to parts of the geological record where the stable isotope compositions of waters are unknown. Moreover, simultaneous determinations of Δ_{47} and $\delta^{18}O$ for carbonates will constrain the $\delta^{18}O$ of water from which they grew.
© 2005 Elsevier Inc. All rights reserved.

1. Introduction

Oxygen isotope exchange equilibria between carbonate minerals and water form the basis of the oldest and most widely used type of geochemical paleothermometer (Urey, 1947; McCrea, 1950; Epstein et al., 1953; Emiliani, 1955, 1966a,b). The carbonate–water thermometer is a landmark of both paleoclimate research and isotope geochemistry, but suffers from one simple but important weakness: the oxygen isotope compositions of both carbonates *and* the waters from which they grew must be known to determine temperature. Carbonates are a widespread and often well-preserved part of the geological record, but only rarely do we have direct and independent evidence for the oxygen isotope compositions of ancient waters.

Various approaches have been taken for resolving or circumventing this difficulty. For example, it is possible to estimate the $\delta^{18}O$ of the ancient ocean by modeling $\delta^{18}O$ gradients in marine sediment pore-waters (Schrag et al., 1996, 2002; Adkins et al., 2002), based on oxygen isotope compositions of benthic foraminifera (Shackleton, 1967), or based on reconstructed sea-level changes and the estimated $\delta^{18}O$ of glacial ice (Dansgaard and Tauber, 1969). These approaches are generally only useful for study of Pleistocene marine records—an important but small subset of all the potential uses of carbonate paleothermometry. Similarly, there are several marine paleothermometers based on speciation of planktonic organisms, relative abundances of alkenones, or the Mg/Ca or Sr/Ca ratios of corals, foraminifera, and other carbonate-producing organisms. These thermometers can also be used to precisely re-construct Pleistocene marine temperature, but are unsuitable for extrapolation in temperature, apply only

to the ocean, and are of uncertain value in the deep geological past.

We present the principles, calibration data and an illustrative application of a new paleothermometer based on 'clumping' of ^{13}C and ^{18}O in the carbonate mineral lattice into bonds with each other—that is, we examine not only the $^{13}C/^{12}C$ and $^{18}O/^{16}O$ ratios of carbonates, but also the fraction of ^{13}C and ^{18}O atoms that are joined together into the same carbonate ion group ($^{13}C^{18}O^{16}O_2^{2-}$). This thermometer is based on a thermodynamically controlled stable isotope exchange equilibrium among components of the carbonate crystal lattice. Because it involves a homogeneous equilibrium (reaction among components of a single phase), it rigorously constrains the temperature of carbonate growth based on the isotopic composition of carbonate alone, independent of the isotopic composition of the water from which it grew or other phases with which it co-exists.

1.1. A paleothermometer based on ordering of ^{13}C and ^{18}O in carbonate minerals

Carbonate minerals contain 20 different isotopologues, or isotopic variants, of the carbonate ion group (Table 1). The most abundant of these, $^{12}C^{16}O_3^{2-}$ (~98.2%) contains no rare isotopes. The next three most abundant, $^{13}C^{16}O_3^{2-}$ (~1.1%), $^{12}C^{18}O^{16}O_2^{2-}$ (~0.6%) and $^{12}C^{17}O^{16}O_2^{2-}$ (~0.11%) are singly substituted (i.e., contain one rare isotope). Collectively, these four isotopologues constitute almost all (~99.99%) of the carbonate ions in natural carbonate minerals, and effectively control their bulk $\delta^{13}C$, $\delta^{17}O$ and $\delta^{18}O$ values. However, most of the isotopic diversity—16 different isotopologues in all—is contained in the doubly, triply and quadrupally substituted carbonate ion units that make up the remaining ~100 ppm. Each of these multiply substituted isotopologues has unique vibrational properties, and therefore they must differ from one another in thermodynamic stability (among other things).

In a carbonate crystal at thermodynamic equilibrium, the relative abundances of the various carbonate ion isotopologues must conform to equilibrium constants for reactions such as:

$$^{13}C^{16}O_3^{2-} + {}^{12}C^{18}O^{16}O_2^{2-} = {}^{13}C^{18}O^{16}O_2^{2-} + {}^{12}C^{16}O_3^{2-}$$
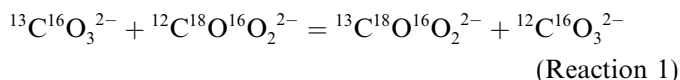
(Reaction 1)

There are many independent reactions of this type, but we focus only on this one because it involves the most abundant (and therefore most easily measured) doubly substituted isotopologue ($^{13}C^{18}O^{16}O_2^{2-}$).

Urey (1947), Bigeleisen and Mayer (1947), and Wang et al. (2004) examine the thermodynamics of reactions analogous to Reaction 1 involving isotopologues of simple molecular gases. They show that equilibrium constants for such reactions are temperature dependent and generally promote 'clumping' of heavy isotopes into bonds with each

Table 1
Abundances of isotopologues of CO_2 and CO_3, assuming bulk $^{13}C/^{12}C$ ratios equal to PDB, bulk $^{18}O/^{17}O/^{16}O$ ratios equal to SMOW, and a stochastic (random) distribution of isotopes

C	Mass	Abundance
Isotopes		
^{12}C	12	98.89%
^{13}C	13	1.11%
O		
^{16}O	16	99.759%
^{17}O	17	370 ppm
^{18}O	18	0.204%

CO_2	Mass	Abundance
Isotopologue		
$^{16}O^{12}C^{16}O$	44	98.40%
$^{16}O^{13}C^{16}O$	45	1.10%
$^{17}O^{12}C^{16}O$	45	730 ppm
$^{18}O^{12}C^{16}O$	46	0.40%
$^{17}O^{13}C^{16}O$	46	8.19 ppm
$^{17}O^{12}C^{17}O$	46	135 ppb
$^{18}O^{13}C^{16}O$	47	45 ppm
$^{17}O^{12}C^{18}O$	47	1.5 ppm
$^{17}O^{13}C^{17}O$	47	1.5 ppb
$^{18}O^{12}C^{18}O$	48	4.1 ppm
$^{17}O^{13}C^{18}O$	48	16.7 ppb
$^{18}O^{13}C^{18}O$	49	46 ppb

CO_3	Mass	Abundance
Isotopologue		
$^{12}C^{16}O^{16}O^{16}O$	60	98.20%
$^{13}C^{16}O^{16}O^{16}O$	61	1.10%
$^{12}C^{17}O^{16}O^{16}O$	61	0.11%
$^{12}C^{18}O^{16}O^{16}O$	62	0.60%
$^{13}C^{17}O^{16}O^{16}O$	62	12 ppm
$^{12}C^{17}O^{17}O^{16}O$	62	405 ppb
$^{13}C^{18}O^{16}O^{16}O$	63	67 ppm
$^{12}C^{17}O^{18}O^{16}O$	63	4.4 ppm
$^{13}C^{17}O^{17}O^{16}O$	63	4.54 ppb
$^{12}C^{17}O^{17}O^{17}O$	63	50 ppt
$^{12}C^{18}O^{18}O^{16}O$	64	12 ppm
$^{13}C^{17}O^{18}O^{16}O$	64	50 ppb
$^{12}C^{17}O^{17}O^{18}O$	64	828 ppt
$^{13}C^{17}O^{17}O^{17}O$	64	0.5 ppt
$^{13}C^{18}O^{18}O^{16}O$	65	138 ppb
$^{12}C^{17}O^{18}O^{18}O$	65	4.5 ppb
$^{13}C^{17}O^{17}O^{18}O$	65	9 ppt
$^{12}C^{18}O^{18}O^{18}O$	66	8 ppb
$^{13}C^{17}O^{18}O^{18}O$	66	51 ppt
$^{13}C^{18}O^{18}O^{18}O$	67	94 ppt

other (increasing the proportions of multiply substituted isotopologues) as temperature decreases. If Reaction 1 follows similar principles, its equilibrium constant should be near 1 at very high temperatures and increase (driving the reaction to the right) with decreasing temperature. Thus, in thermodynamically equilibrated carbonates, the equilibrium constant for Reaction 1 can serve as the basis of a geothermometer, provided that the temperature dependence of this reaction is known and the abundances of all the reactant and product isotopic species can be measured.

Reaction 1 can be thought of as analogous to order/disorder exchange reactions among cation sites in pyroxenes

and feldspars (e.g., Myers et al., 1998). For this reason, we describe the thermometer based on Reaction 1 as the '13C–18O order/disorder carbonate thermometer'. A less precise, but less ungainly term we also use here is the 'carbonate clumped-isotope thermometer'. The important feature of this thermometer is that it involves a homogeneous equilibrium (that is, a reaction among components of one phase, rather than between two or more phases), and therefore rigorously constrains temperature without knowing the isotopic composition of a second phase.

We are aware of no way one could directly measure abundances of $^{13}C^{18}O^{16}O_2^{2-}$ ionic groups in carbonate minerals with sufficient precision to be useful for paleothermometry. They make up only ca. 60 ppm of natural carbonates (Table 1), and we show below that they must be analyzed with relative precision of ca. 10^{-5}. It seems unlikely that any spectroscopic method could meet these requirements. However, Eiler and Schauble (2004) and Affek and Eiler (2005), recently showed that it is possible to analyze $^{13}C^{18}O^{16}O$ in CO_2 at natural abundances and with the necessary precision. We show here that the abundance of $^{13}C^{18}O^{16}O$ in CO_2 produced by phosphoric acid digestion of carbonate minerals is proportional to the abundance of $^{13}C^{18}O^{16}O_2^{2-}$ ionic groups in those minerals themselves. Thus, combination of the mass-spectrometric methods of Eiler and Schauble (2004) and Affek and Eiler (2006) with long-established methods of phosphoric acid digestion of carbonates can constrain the equilibrium constant for Reaction 1, and therefore the growth temperature, in a sample of solid carbonate.

2. Samples and methods

2.1. Samples

2.1.1. Natural and synthetic calcite standards

We studied one inter-laboratory calcite standard (NBS-19, distributed by the IAEA) and three intra-laboratory calcite standards, 'MARJ-1', 'MZ carbonate' and 'Sigma-carb'. Two of the standards (NBS-19 and MARJ-1) were purified from Italian Carrara marbles that were metamorphosed to upper-greenschist facies during the mid-Tertiary (Friedman et al., 1982; Molli et al., 2000; Leiss and Molli, 2003; Ghosh et al., 2005). MAR-J1 studied here has a grain size of less than 250 μm and a texture and chemical and O and C isotope composition similar to NBS-19 (Ghosh et al., 2005). The MZ carbonate standard was obtained from MERCK (http://chemdat.merck.de/) and the Sigma-carb standard was obtained from Sigma–Aldrich chemical supply (http://www.sigmaaldrich.com/). Both of these carbonates were produced by passing carbon dioxide through a slurry of calcium oxide and water, producing a very fine precipitate of calcite (the industrial term for this reaction is the 'carbonation process'). The typical grain size of these carbonate powders is 40–50 μ, based on measurement under a binocular microscope. It is unimportant for our purposes whether the carbonation process promotes

oxygen isotope exchange equilibrium between carbonate and water; it is important only that the carbonate precipitates are chemically pure and isotopically homogeneous when sampled in mg-sized aliquots, and thus provide a useful basis for establishing the precision of our analyses.

2.1.2. Equatorial surface coral

We examined a sample of *Porites* surface coral collected from the west shore of Sumatra in the equatorial Indian Ocean. This specimen, Mm97Bc, was obtained from K. Sieh and was collected from the crest of a living coral head in 1 m water depth at Memong Island (98.54 E; 0.035 N) (Natawidjaja, 2003, 2004). We estimate the mean growth temperature of this coral to be 29.3 ± 2 °C, based on instrumental records from this region, which is characterized by a weak seasonality and little spatial variability over hundreds of km (Abram et al., 2003). Additional information about this sample can be found in (Natawidjaja, 2003). This aragonitic coral slab (1–2 cm) was sampled using a file, yielding ~100 μm powder.

2.1.3. Deep sea coral

We examined two specimens of *D. dianthus* (a deep sea coral also previously referred to as *D. cristagalli*). Sample 47407, described in Adkins et al. (2003), was collected at 549 m water depth in the Southern Pacific ocean (54.49 S, 129.48 W) and grew at an estimated average temperature of 5.5 ± 1.0 °C, based on instrument records from similar depth and location. Sample 47413 was collected at 420 m water depth off the south shore of New Zealand (50.38 S, 167.38 E) and grew at an estimated average temperature of 8.0 ± 0.5 °C, also based on local instrument records. These aragonitic corals were sampled by breaking off fragments of their fragile septa, followed by crushing to a mean grain size of 100 μm. Both samples are from the Smithsonian collections.

2.1.4. Calcites grown inorganically at known temperature

We grew calcite by removing CO_2 from aqueous solutions of sodium bicarbonate and calcium chloride or from calcite-saturated solutions, using a method similar to that described by Kim and O'Neil (1997). Two different variants of this method were employed:

(1) Sample HA1 was prepared in the following way: first, CO_2 (99.96%, Air Liquide) was bubbled through de-ionized water at room temperature for 1 h. Next, $NaHCO_3$ (AR, Mallickrodt) was added to the acidified water in quantities required to produce a 5 mM solution (ΣCO_3^{2-}). After complete dissolution of $NaHCO_3$, $CaCl_2$ (99.8%, Fisher scientific) was added to the solution, in amounts required to make an equimolar $NaHCO_3$:$CaCl_2$ solution, and the solution was stirred to complete dissolution. CO_2 was then removed from this solution using methods described below, forcing

precipitation of calcite. The yield of calcite from this experiment was low, and so we modified our procedure for the remaining experiments.

(2) The rest of the samples were prepared by first bubbling CO_2 into a stirred suspension of $CaCO_3$ (99% pure obtained from Sigma–Aldrich chemical supply, approximately 0.5 g in 800 ml de-ionized water) for 1–2 h. The un-dissolved $CaCO_3$ was removed by gravitational filtering through a grade-2 Whatman filter. The solution was then purged of CO_2 as described below, forcing precipitation of calcite. Solutions prepared in this way yielded far more calcite per unit time, perhaps because partly dissolved nuclei of starting calcite remained in suspension, providing templates for calcite precipitation.

Regardless of the way the solution was prepared, once ready, approximately 200 ml was poured into an Erlenmeyer flask that was sealed with a rubber stopper equipped with inlet and outlet BEV-A-LINE tubing. This was placed in a controlled-temperature water bath and allowed to thermally equilibrate for 1 h. The temperature in the water bath was monitored throughout our experiment using a mercury thermometer. The temperature stability of the chilled bath was $\pm 0.2\,°C$, that of the room temperature bath was $\pm 1\,°C$, and that of heated water bath was $\pm 2\,°C$. After thermally equilibrating, N_2 gas (99.96%, Air Liquide) was bubbled first through a similar Erlenmeyer flask filled with the same de-ionized water used to make our solution (to minimize isotopic evolution of the solution due to evaporation into the N_2 gas stream) and then through the solution itself through a Pasteur pipette dipped in the solution and attached to the rubber stopper sealing the Erlenmeyer flask. The N_2 flow rate was approximately 10 ml/min for samples HA1 through HA7 and HA12 and approximately 50 ml/min for sample HA9. Carbon dioxide dissolved in the solution partitioned into the N_2 and was removed from the system, promoting super saturation and slow precipitation of calcium carbonates (Fig. 1, panel 1). The bubbling rate of N_2 was controlled by a regulator attached to the gas cylinder and was monitored by counting the number of bubbles per 30 s (10 ml/min was equivalent to about 20 bubbles to 30 s).

Precipitation experiments were performed at room temperatures ($23 \pm 1\,°C$), in an ice–water bath temperature ($1 \pm 0.2\,°C$), and in heated water baths (at 33 ± 2 and $50 \pm 2\,°C$). The time required for the first appearance of visible precipitate depended on the composition of the solu-
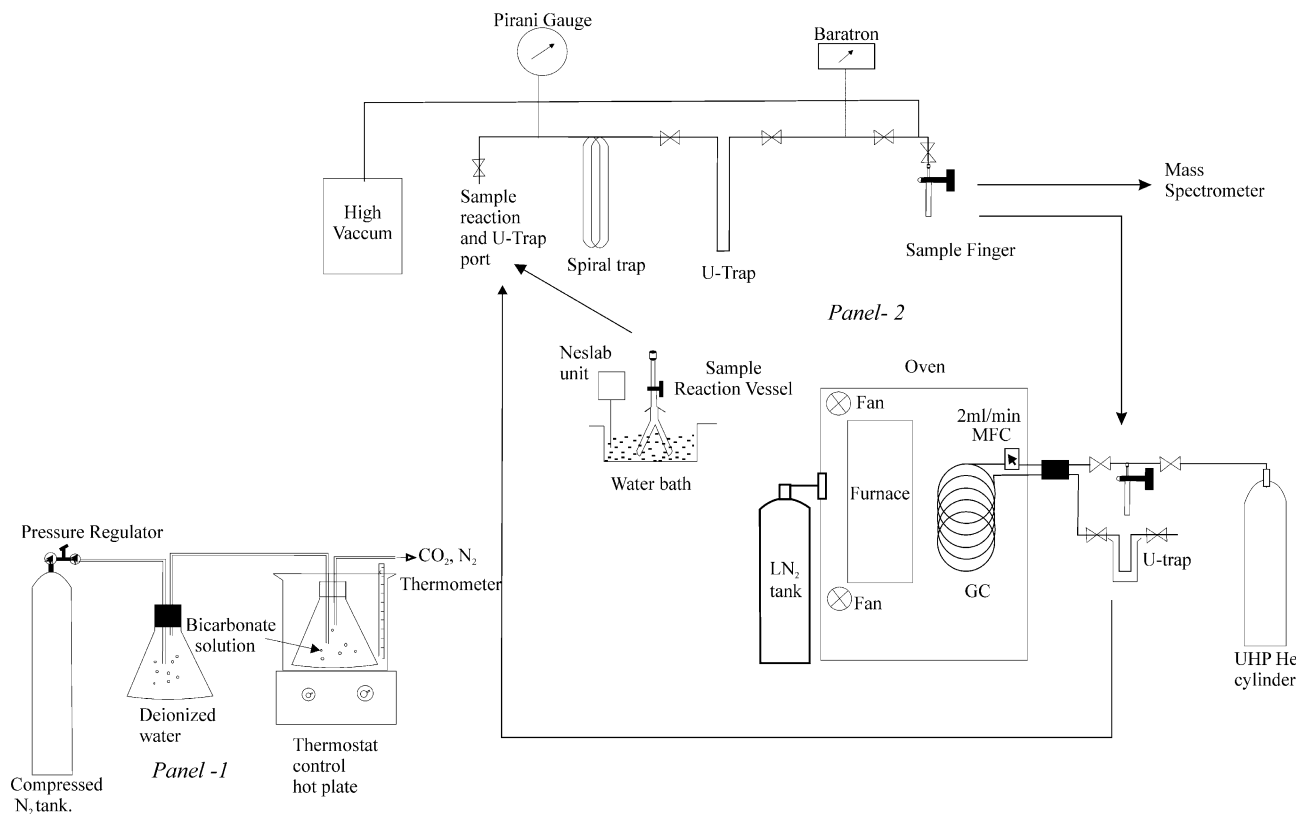

Fig. 1. Schematic illustration of apparatus used in this study. Panel 1: System of vessels and purge gases used in the synthesis of calcite from bicarbonate solutions. See text for explanation. Panel 2: vacuum and carrier-gas apparatus used for phosphoric acid digestion of carbonate and clean-up of product CO_2. Powdered carbonate sample and phosphoric acid are placed in separate arms of the reaction vessel, evacuated, placed in a constant-temperature bath, and then the vessel is tipped to mix acid with sample. Product CO_2 is cryogenically purified of water and other trace gases, condensed into a small glass vessel, and transferred to the carrier-gas system for further purification. There, CO_2 is entrained in a He stream flowing at 2 ml/min, passed through a 32 m long 530 μm ID Supelco gas-chromatography column held at $-10\,°C$ and re-collected in a glass trap immersed in liquid nitrogen. Finally, the re-collected CO_2 is returned to the vacuum system and cryogenically separated from He purge gas prior to mass spectrometric analysis.

tion, temperature, and bubbling rate, and was typically about 1 day. It took at least one day and a maximum of five days to generate sufficient material ($\sim$10 mg CaCO$_3$) for both X-ray diffraction and isotopic analysis. Upon completion of each experiment, the solid carbonate precipitated on the walls and at the bottom of the vessel was removed using a rubber spatula, filtered by injecting the suspension through a Whatman GF/C filter paper and then air dried for at least 48 h prior to storage for isotopic analysis.

The mineralogy of every precipitate was identified by X-ray diffraction analysis and some of the precipitates were examined by optical microscopy. Further details about each sample are summarized in Table 5.

An aliquot (15–10 ml) of the supernatant was stored in an air-tight polypropylene container for $\delta^{18}O$ analysis using a GasBench II water-equilibration system attached to a Thermo Finnegan Delta Plus located at University of California Irvine, with analytical precision of $\pm$ 0.1‰. The differences in $\delta^{18}O$ between calcites and waters (see Table 5 and the Results and Discussion, below) fall broadly within the range previously observed for inorganic calcite synthesis experiments such as the ones we performed (O'Neil et al., 1969; Kim and O'Neil, 1997), but do not agree exactly (the average disagreement in the difference ($\delta^{18}O_{carbonate} - \delta^{18}O_{water}$) is 0.3‰). This disagreement could reflect any combination of: temperature variations during experiments; failure to maintain a constant isotopic composition of solution during experiments or between sampling and final analyses; and analytical errors in determinations of the $\delta^{18}O$ of water and carbonate. All of these factors potentially apply both to our experiments and those to which we compare our results. Variations and errors in temperature influence the accuracy of our calibration of Reaction 1, but the other factors should not (see Fig. 4 in the Section 3, below). We do not believe we can independently determine which combination of these errors in our experiments and those of Kim and O'Neil (1997), explains this discrepancy between the two studies. However, its magnitude translates into a discrepancy in apparent temperature of only 2 °C. This is comparable to the precision in temperature corresponding to our best analytical precision in Δ_{47}, and thus any error in our experiments implied by this comparison seems unlikely to introduce a significant additional error in the thermometer based on Reaction 1.

2.2. Phosphoric acid digestion of carbonates

We extracted CO$_2$ from carbonates by reaction with anhydrous phosphoric acid, following the methods of McCrea (1950) and Swart et al. (1991). Fig. 1 (panel 2) illustrates the glass vacuum apparatus used for this purpose. This apparatus uses McCrea-type reaction vessels and conventional vacuum cryogenic procedures to trap product CO$_2$ and separate it from trace water. We imagine that more sophisticated, automated devices should also be appropriate for analyses such as those we describe, although large samples (ca. 5 mg) are preferred to generate the intense mass-47 ion beams needed for precise isotopic analyses, and not all such systems can easily accommodate such large samples. The details of our phosphoric acid digestion procedure are as follows:

- Each reaction vessel is loaded with ca. 5 mg of sample and 10 ml of $\sim$103% phosphoric acid (density 1.90 g/ml) and evacuated to a baseline pressure of $\sim$4 × 10^{-3} mbar for more than 2 h.
- Each reaction vessel is then immersed a NESLAB water bath, held at a temperature of 25 °C (unless otherwise noted), and allowed to thermally equilibrate for 1 h prior to tipping the acid reservoir to spill over the sample powder, starting the acid digestion reaction.
- Unless otherwise noted, the reaction is allowed to proceed for at least 12 h and usually ca. 16 h (over night).
- Product CO$_2$ is then cryogenically collected into a glass trap immersed in liquid nitrogen, and then released by warming the trap to $-$77.8 °C (by immersing the trap in a dry ice + ethanol slurry), leaving any trace water frozen in the trap.
- Product CO$_2$ is then cryogenically collected into a small ($\sim$1 cc) evacuated glass sample vessel.

2.3. Purification of analyte CO$_2$

Multiply substituted isotopologues make up a small fraction (10's of ppm at most) of CO$_2$ having natural stable isotope abundances, and so accurate analysis requires a virtual absence of isobaric interferences from contaminant gases (Eiler and Schauble, 2004). The most important of these contaminants are hydrocarbons and halocarbons (Eiler and Schauble, 2004). These are most easily removed by gas-chromatography, and can be monitored in all samples by simultaneous analysis of masses 47, 48 and 49. These contaminants typically contribute nearly equally to all three of these masses, producing distinctive and highly correlated relationships between relatively small 47 excess (tenth's of per mil) and proportionately greater excesses in 48 (several per mil) and 49 (tens of percent; Eiler and Schauble, 2004). Therefore, each CO$_2$ sample analyzed in this study was entrained in a He stream flowing at 2 ml/min and passed through a 30 m long 530 μm ID Supelco gas-chromatography column packed with porous divinyl benzene polymer held at $-$10 °C, and re-collected in a glass trap immersed in liquid nitrogen. The gas-chromatography column was held in an oven (Hewlet Packard instruments Model description: Perfect fit Model no: G1530A), modified so that it could be purged with the boil-off gas from a tank of liquid nitrogen. See Fig. 1, panel 2 for further details. For these conditions and our typical sample size (ca. 50 μmol), elution times are 1 h with collection efficiency of >95%. Small variations in collection efficiency within this range appear not to be associated with isotopic fraction-

ation. Finally, the re-collected CO_2 was then cryogenically separated from He purge gas by condensation in a glass trap immersed in liquid nitrogen followed by evacuation of the residual He. Finally, the purified CO_2 was condensed back into the small glass sample container and introduced to the dual-inlet system of a Finnigan MAT 253 isotope ratio mass spectrometer (see below). If evidence of contamination was observed during analysis (based on correlated 47, 48 and 49 signals and/or atypical drift in the analysis), the entire procedure was repeated to further purify the sample. The GC column and connection assembly was baked at 200 °C at a He flow rate of 5 ml/min for more than 30 min between samples.

2.4. Mass spectrometric analyses of purified CO_2

All analyses reported here were made on a Finnigan MAT 253 gas source isotope ratio mass spectrometer, configured to simultaneously collect ion beams corresponding to $M/Z = 44$, 45 and 46 (read through $3 \cdot 10^8$ to $1 \cdot 10^{11}$ Ω resistors), as well as 47, 48 and 49 (read through 10^{12} Ω resistors). All measurements were made in dual inlet mode, and with a typical source pressure sufficient to maintain the mass-44 ion beam at a current of 160 nA. Each analysis involves 10 cycles of sample-standard comparison and each cycle involves 8 s integration of sample and standard ion beams. Analyses were standardized by comparison with an intra-laboratory reference gas whose bulk composition had been previously calibrated against CO_2 produced by phosphoric acid digestion of NBS-19, and whose abundance of mass-47 isotopologues was established by comparison with CO_2 that had been heated to 1000 °C to achieve the stochastic distribution. These heated gas standards were prepared to have bulk stable isotope compositions similar to those of unknowns, in order to minimize the potential errors associated with mass spectrometric nonlinearities (which are observable when samples and standards differ by more than ca. 20–30‰ in any given isotope ratio). See Eiler and Schauble (2004) for further details regarding protocols for standardizing measurements of mass 47 CO_2.

Abundances of mass-47 CO_2 are reported using the variable Δ_{47}, defined as in Eiler and Schauble (2004) and Wang et al. (2004). Briefly, the Δ_{47} value is the difference in per mil between the measured 47/44 ratio of the sample and the 47/44 ratio expected for that sample if its stable carbon and oxygen isotopes were randomly distributed among all isotopologues—a case described as the stochastic distribution. External precision of individual measurements of Δ_{47} is typically 0.03‰, consistent with counting-statistics limits for these ion intensities and analytical durations. Most samples were measured 3–10 times, such that the standard error of their Δ_{47} values is in the range 0.01–0.02‰.

Finally, we define here the variable $\Delta_{^{13}C^{18}O^{16}O_2}$. By analogy with Δ_{47} for CO_2, $\Delta_{^{13}C^{18}O^{16}O_2}$ equals the deviation, in per mil, of the abundance of $^{13}C^{18}O^{16}O_2^{2-}$ carbonate ion units in a carbonate crystal from the abundance expected for the stochastic distribution of all stable isotopes in that crystal. To first order, $\Delta_{^{13}C^{18}O^{16}O_2}$ equals $k_{eq}{}^1$ (the equilibrium constant for Reaction 1), -1×1000.

3. Results

3.1. External precision of CO_2 extracted at 25 °C from carbonate standards

Fig. 2 plots all analyses of the NBS-19, MAR-J1, MZ carbonate and Sigma-carb standards made between January, 2004 and April, 2005. Each data point represents the average of between 1 and 10 analyses of the gas from a single acid extraction experiment; the error bar is ± 1se (the standard error for that group of analyses—the appropriate statistic to evaluate the reproducibility of separate acid extraction experiments).

Carbon dioxide extracted from NBS-19 was analyzed eight times where each gas was analyzed 4 or more times (so that the standard error for each sample is expected to be ca. 0.015‰). These yield an average and standard devi-
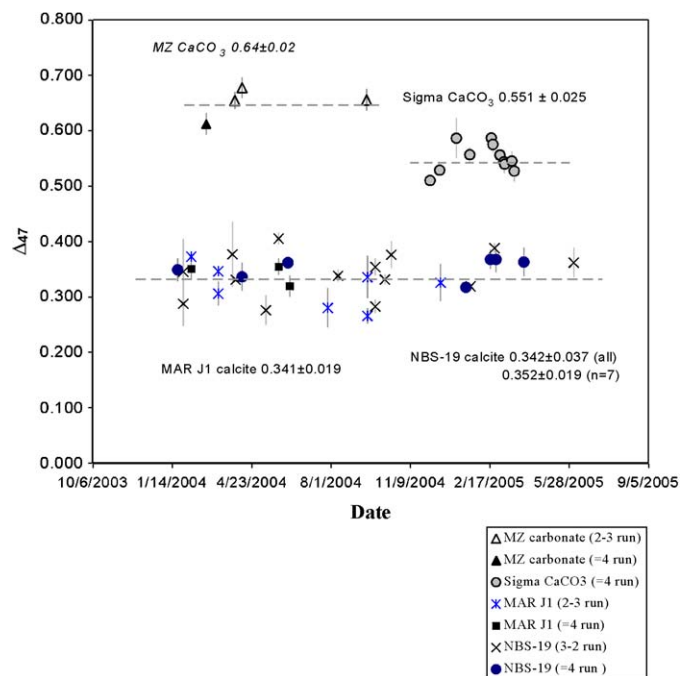
Fig. 2. Values of Δ_{47} determined for CO_2 extracted from reference carbonates, NBS-19, MAR J1, MZ carbonate and Sigma carb., between January 2004 and April 2005 (see Table 2). Each data point represents the average of between 1 and 10 analyses of the gas from a single acid extraction experiment. The error bar for each point is ± 1SE (the standard error for that group of replicate mass-spectrometric analyses of a single gas sample). This standard error obviously shrinks with increasing numbers of replicate mass spectrometric analyses; this fact is visually emphasized by using different symbols to discriminate between samples analyzed, 2–3 times, or 4 or more times. We exclude samples analyzed only once for visual clarity; all are shown as small symbols, and have average standard errors of ± 0.030 ‰, 1SE. Long-term analytical reproducibility is generally a small multiple (1× to 1.5×) of that expected by counting statistics alone. See text for discussion.

ation for their Δ_{47} values of 0.341 ± 0.034 (Table 2). One of these eight samples (the Δ_{47} value of 0.27, measured on 9/29/2004) is a 2σ outlier to the rest of the group; the remaining 7 have an average and standard deviation of 0.352 ± 0.019—the expected reproducibility based on counting statistics alone. There is no obvious reason why the measurement on 9/29/2004 is an outlier to this population, although our sample purification procedures have improved through time and we suspect data generated before 11/2004 are more prone to unidentified contaminants than those generated after. Three samples of CO_2 from MAR-J1 were analyzed 4 or more times each, and yielded an average and standard deviation for Δ_{47} of 0.341 ± 0.019 (Table 2). NBS-19 and MAR-J1 are both Italian marbles, and so we find it unsurprising that their Δ_{47} values are indistinguishable from each other. Table 2 and Fig. 2 also present analyses of CO_2 samples extracted from these materials where each gas was analyzed only 1, 2 or 3 times each. These data are similar to the measurements summarized above, but scatter more widely (ca. $\pm 0.03\%_0$, 1σ), as expected for their poorer counting statistics. Curiously, the mean Δ_{47} values for CO_2 analyzed fewer than 4 times are slightly lower than those analyzed four or more times for two of three standards for which such a comparison can be made (NBS-19 and MAR-JI, but not MZ carbonate). We suspect that this reflects a difference in standardization and/or trace contamination between relatively early generated data (prior to 6/2004, most of which were analyzed 1–3 times and were less carefully cleaned) and more recent data (most of which are analyzed 4 or more times and were more carefully cleaned).

Eleven samples of CO_2 from Sigma-carb standard were measured where each gas was analyzed 4 or more times. These yield an average and standard deviation for Δ_{47} of 0.551 ± 0.025. This reproducibility is poorer than expected from counting statistics alone (ca. ± 0.01–$0.02\ \%_0$), but the variation of observed values through time makes it evident that external precision over short time periods (weeks) is systematically better: When data are grouped by week, the sample-to-sample standard deviations are 0.005, 0.009, 0.016 and 0.035 (see Table 2)—i.e., the average external precision for data measured the same week (± 0.015) is equal to that expected from counting statistics. This grouping of data over short time periods is also evident in Fig. 2, where one can see that measurements of Sigma-carb standard drift by ca. 0.01–0.03‰ over several-week timescales rather than being randomly distributed over their 4 months interval. We suspect this is evidence that the external precisions of our acid extraction measurements are comparable to counting statistics (0.01–0.02‰) over short time periods, but that some aspect of our measurements, such as mass spectrometer calibration and/or the temperature or cleanliness of acid extraction, drifts subtly from week to week. Finally, only one measurement of CO_2 from MZ standard involved 4 or more analyses of product CO_2. However, the group of all samples (most of which were analyzed only 1–3 times) over a 3 month period

Table 2
Stable isotope analyses, including Δ_{47}, of CO_2 extracted by phosphoric acid digestion at 25 °C from various inter- and intra-laboratory carbonate standards

Date	Run no.*	$\delta^{13}C_{PDB}$	$\delta^{18}O_{SMOW}$	Δ_{47}	Standard error
NBS-19					
Number of run $\geqslant 4$					
1/21/2004	A 1533–38	1.92	38.83	0.35	0.02
4/11/2004	A 2166–70	1.97	38.90	0.34	0.03
6/8/2004	B 123–26	1.95	39.04	0.36	0.01
9/29/2004	B 505–511	1.93	38.78	0.27	0.01
1/18/2005	C 325–29	2.01	38.20	0.32	0.01
2/18/2005	C 913–917	1.99	39.30	0.37	0.02
2/25/2005	C 1092–95	2.00	39.38	0.37	0.02
4/1/2005	C 1585–88	1.99	39.27	0.36	0.03
Number of run 3-2					
1/28/2004	A 1573–74	2.00	38.97	0.35	0.06
1/28/2004	A 1575–76	2.02	39.00	0.29	0.04
3/30/2004	A 2084–85	1.95	38.96	0.38	0.06
4/3/2004	A 2142–43	1.96	38.92	0.33	0.003
5/11/2004	B 2263–64	1.94	39.08	0.28	0.03
5/27/2004	B 2471–73	1.89	38.94	0.41	0.01
8/10/2004	B 176–77	2.01	39.14	0.34	0.01
9/26/2004	B 450–52	1.87	39.10	0.28	0.01
9/26/2004	B 453–55	1.96	39.23	0.35	0.02
10/8/2004	B 665–68	1.92	39.58	0.33	0.01
10/16/2004	B 744–47	1.75	38.86	0.38	0.02
1/24/2005	C 497–500	1.96	39.23	0.32	0.00
2/23/2005	C 1463–65	1.99	39.05	0.39	0.01
6/3/2005	C 1979–81	1.69	38.89	0.36	0.03
Single run					
1/28/2004	A 1561	1.97	38.82	0.47	—
2/2/2004	A 1620	1.98	38.96	0.20	—
2/3/2004	A 1632	2.01	38.98	0.21	—
2/15/2004	A 1762	2.05	39.02	0.29	—
2/18/2004	A 1804	1.93	38.65	0.23	—
3/9/2004	A 1924	1.96	38.83	0.28	—
3/30/2004	A 2087	1.96	38.99	0.26	—
3/30/2004	A 2040	1.97	39.01	0.39	—
4/20/2004	A 2197	1.91	38.70	0.34	—
5/11/2004	B 2268	1.99	39.13	0.24	—
5/14/2004	B 2313	1.99	39.13	0.32	—
5/19/2004	B 2363	1.94	39.08	0.36	—
5/25/2004	B 2441	1.94	39.04	0.43	—
MAR J1					
Number of run $\geqslant 4$					
2/7/2004	B 2851–53	2.01	39.20	0.35	0.02
5/27/2004	B 2854–57	1.97	39.26	0.35	0.02
6/10/2004	B 583–87	1.96	39.29	0.32	0.02
Number of run 3-2					
2/7/2004	B 2855–56	1.93	39.15	0.37	0.01
3/12/2004	B 1440–43	2.02	39.37	0.31	0.02
3/12/2004	B 1342–44	1.90	38.67	0.35	0.01
7/28/2004	B 41–42	1.92	39.00	0.28	0.04
9/16/2004	B 371–73	1.95	39.08	0.27	0.01
9/16/2004	B 374–76	1.95	39.06	0.34	0.04
12/17/2004	B 1443–45	1.92	39.20	0.33	0.03
Single run					
9/17/2004	B 368	1.945	39.08	0.27	—
Sigma carbonate					
Number of run $\geqslant 4$					
12/4/2004	B 1389–99	−42.31	20.76	0.51	0.01

Table 2 (continued)

Date	Run no.*	$\delta^{13}C_{PDB}$	$\delta^{18}O_{SMOW}$	Δ_{47}	Standard error
12/16/2004	B 1402–13	−42.32	20.73	0.53	0.01
1/6/2005	B 171–72	−42.46	20.77	0.59	0.04
1/23/2005	C 460–63	−42.48	20.44	0.56	0.01
2/19/2005	C 933–38	−42.28	20.95	0.59	0.01
2/21/2005	C 963–68	−42.52	20.57	0.58	0.01
3/2/2005	C 1137–42	−42.06	20.94	0.56	0.01
3/7/2005	C 1214–19	−42.02	20.88	0.54	0.02
3/8/2005	C 1263–68	−42.32	20.86	0.54	0.02
3/17/2005	C 1379–84	−42.37	20.71	0.55	0.02
3/20/2005	C 1415–20	−42.28	20.95	0.53	0.02
MZ carbonate					
Number of run ⩾ 4					
2/26/2004	A 1853–56	−13.29	35.63	0.61	0.008
Number of run 3–2					
4/11/2004	A 2171–72	−13.44	35.33	0.68	0.019
4/2/2004	A 2124–25	−13.44	35.30	0.65	0.016
9/15/2004	B 359–361	−13.56	35.03	0.66	0.020
Single run					
2/15/2004	A 1763	−13.48	35.35	0.65	—
5/11/2004	A 2261	−13.32	35.48	0.63	—
4/7/2004	A 2140	−13.43	35.35	0.67	—
4/7/2004	A 2128	−13.49	35.34	0.61	—
3/9/2004	A 1983	−13.41	35.24	0.63	—

yields an average and standard deviation for Δ_{47} of 0.64 ± 0.02; the precision of these data is indistinguishable from the expected limits from counting statistics (± 0.02–0.03 for these data).

These data indicate that long-term external precision in analyses of Δ_{47} for CO_2 produced from acid digestion of carbonates is similar to counting statistics (± 0.01–0.02) over short time periods (days to weeks), but can degrade to twice the counting statistics limit ($\pm 0.03‰$) over periods of months. One implication of this result is that the precision for Δ_{47} measurements of unknowns should be maximized by normalization to a carbonate standard measured within the same week under the same conditions.

3.2. Effects of varying the temperature of phosphoric acid digestion

In the absence of any analytical fractionation, the Δ_{47} value of CO_2 produced by carbonate acid digestion should equal the $\Delta_{13C^{18}O^{16}O_2}$ value of reactant carbonate (this is easily shown by sampling statistics; see Table 1). However, reaction of carbonate with phosphoric acid releases only 2/3 of the carbonate oxygen as CO_2; the remainder remains in solution. This reaction is accompanied by an oxygen isotope fractionation, yielding CO_2 that is ca. 10‰ higher in $\delta^{18}O$ than reactant carbonate. The exact magnitude of this fractionation varies with reaction temperature and differs among the various carbonate minerals (Sharma and Clayton, 1965; Swart et al., 1991; Kim and O'Neil, 1997). The physical cause of this fractionation is unclear. It might reflect a temperature-dependent exchange equilibrium between extracted CO_2 and residual O in solution, in which

case the Δ_{47} value of product CO_2 should equal the equilibrium value for gaseous CO_2 at the temperature of extraction (Wang et al., 2004; Eiler and Schauble, 2004) and no information regarding ordering of ^{13}C and ^{18}O in the carbonate mineral lattice should be preserved. It might instead reflect a kinetic isotope effect acting on the C–O bond; in this case we expect that $\alpha^{18O}_{CO_2-CO_3^{2-}}$ should differ for ^{13}C and ^{12}C carbonate ions, and Δ_{47} of extracted CO_2 should be proportional but not equal to $\Delta_{13C^{18}O^{16}O_2}$. We expect that in this case any offset between $\Delta_{13C^{18}O^{16}O_2}$ and Δ_{47} should vary with extraction temperature, because $\alpha^{18O}_{CO_2-CO_3^{2-}}$ varies with temperature. If the physical cause is a kinetic isotope effect acting on metal-O bonds, we expect that there should be little or no sensitivity to ^{13}C–^{12}C substitution, and Δ_{47} of product CO_2 should equal or closely approach $\Delta_{13C^{18}O^{16}O_2}$.

We extracted CO_2 from Sigma-carb standard at 25, 50 and 80 °C and from NBS-19 at 25, 35 and 45 °C. Table 3 and Fig. 3 summarize results of these experiments. The NBS-19 data discussed here were generated very early in this study and lacked the careful purification, standardization and replication characteristic of other data in this paper; they cannot be directly compared with NBS-19 data in Table 2 and Fig. 2. However, they do provide useful constraints on the temperature effect on acid digestion fractionations and so are included here. The $\delta^{18}O$ value of product CO_2 decreases with increasing reaction temperature, with an average slope of $-0.028‰$ per °C (Table 3; this slope is similar to that found by Swart et al., 1991). Also as expected, the $\delta^{13}C$ value of product CO_2 is similar at all reaction temperatures. The Δ_{47} value of product CO_2 decreases with increasing reaction temperature with an overall slope of $-0.0016‰$ per °C. The results of these experiments are inconsistent with an exchange equilibrium between extracted CO_2 and residual oxygen because the Δ_{47} value of product CO_2 is far from the internal equilibrium for CO_2 gas at the temperatures of extraction (which varies from Δ_{47} of 0.93‰ at 25 °C to 0.64‰ at 80 °C; Wang et al., 2004; Eiler and Schauble, 2004). Thus, these results suggest that the Δ_{47} value of CO_2 produced by acid digestion of carbonate has some simple proportionality to the $\Delta_{13C^{18}O^{16}O_2}$ value of that carbonate, and that this proportionality is only weakly dependent on reaction temperature.

Table 3
Stable isotope compositions of CO_2 released from NBS-19 and Sigma carbonate reacted at three different temperature with 103% phosphoric acid

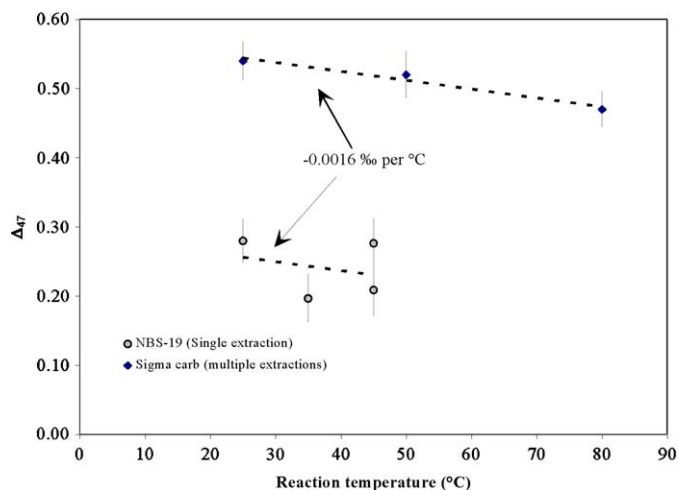| Sample	$\delta^{13}C_{PDB}$	$\delta^{18}O_{SMOW}$	Temperature of reaction (°C)	Δ_{47}	Standard error of Δ_{47} values
NBS-19	1.95	39.00	25	0.28	0.032
NBS-19	2.01	38.61	35	0.197	0.035
NBS-19	1.97	38.29	45	0.21	0.038
NBS-19	1.96	38.09	45	0.28	0.036
Sigma carb	−42.31	20.76	25	0.54	0.028
Sigma carb	−42.28	19.81	50	0.52	0.034
Sigma carb	−42.20	19.22	80	0.47	0.026

Fig. 3. Values Δ_{47} for CO_2 extracted from Sigma-carb and NBS-19 standards at 25, 35, 45, 50 and 80 °C. The $\delta^{18}O$ value of product CO_2 decreases with increasing reaction temperature, with an average slope of $-0.028‰$ per °C (see Table 3; this slope is similar to that found by Swart et al., 1991). The Δ_{47} value of product CO_2 decreases with increase in reaction temperature, with an overall slope of $-0.0016‰$ per °C. Note that NBS-19 analyses were made early in this study and lack the standardization, purification and replication of other data; they cannot be directly compared to measurements of NBS-19 summarized in Table 2.

3.3. Analyses of carbonates subjected to high-temperature re-crystallization

Aliquots of MZ and Sigma-carb standards and an aragonitic deep sea coral (47413) were re-crystallized by loading them into a sealed Pt capsule and heating to 1100 °C for 48 h in a TZM (Tungsten Zirconium Molybdenum alloy) cold-seal pressure vessel under 1000 bars of pressure. Experimental charges were quenched in air at the end of each experiment. The recovered calcite crystals were examined under the binocular and petrographic microscopes and showed evidence of pervasive re-crystallization and coarsening.

This high-temperature re-crystallization procedure should drive Reaction 1 toward a stochastic distribution. Thus, if acid digestion produces no difference between $\Delta_{13C^{18}O^{16}O_2}$ and Δ_{47}, we should find that CO_2 extracted from these materials has a Δ_{47} value of $0‰$. If we find some other result, it could indicate a fractionation of associated with acid digestion (as was suggested in the last section by the dependence of Δ_{47} values on extraction temperature).

Table 4 and Fig. 4 summarize the results of analyses of CO_2 produced by acid digestion of these materials. We
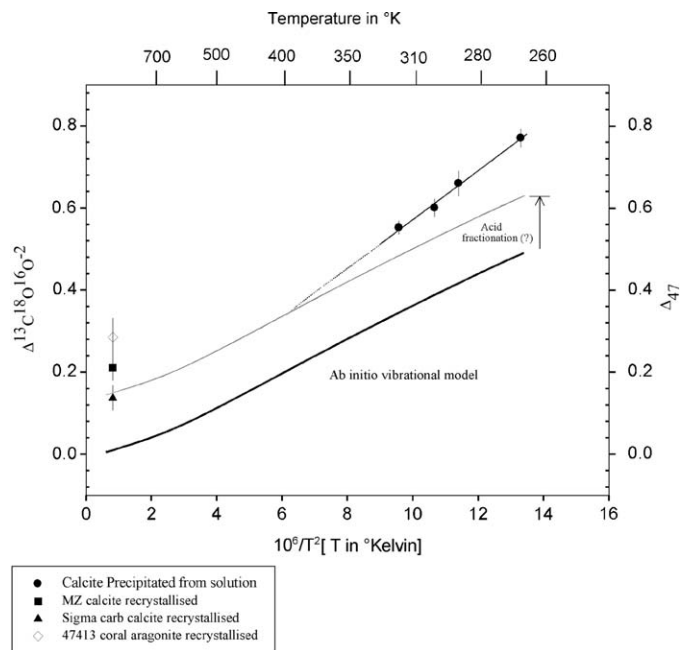

Fig. 4. Plot of the $\Delta_{13C^{18}O^{16}O_2}$ value (approximately equal to $1000 \cdot (k_1 - 1)$, where k_1 is the equilibrium constant of Reaction 1), as predicted by Schauble and Eiler (2004); (left vertical scale; solid curve) and the Δ_{47} value of CO_2 extracted from re-crystallized and synthetic calcites (see legend), vs. $10^6/T^2$. All data are averages of multiple extractions, where appropriate (see Tables 4 and 5). Note that in the absence of any acid-digestion fractionation Δ_{47} of CO_2 extracted from carbonate minerals should equal $\Delta_{13C^{18}O^{16}O_2}$ of reactant carbonate. Calcite and aragonite recrystallized at high temperature are expected to yield CO_2 with Δ_{47} near 0, and thus the higher observed values suggest an acid digestion fractionation of ca. 0.1–0.2‰ (a value of $\leqslant 0.14‰$ is preferred, for reasons discussed in the text). The gray curve illustrates the Schauble and Eiler (2004) model estimate for $\Delta_{13C^{18}O^{16}O_2}$ offset by this amount. The data for calcites grown from aqueous solution show a correlation ($r = 0.94$) between Δ_{47} of extracted CO_2 and T^{-2}, where T is the growth temperature in Kelvin. This correlation line is shown as a thin black line. The dashed extension of this line to lower values of $10^6/T^2$ is our hypothesis for the relationship between carbonate growth temperature and Δ_{47} of extracted CO_2 at temperatures greater than 50 °C.

find they yield CO_2 with Δ_{47} values of 0.14 ± 0.03 (for re-crystallized Sigma-carb standard), 0.22 ± 0.03 (for re-crystallized MZ standard), and 0.25 ± 0.02 (for deep sea coral 47413). These data suggest that CO_2 produced by phosphoric acid digestion at 25 °C is subtly (~0.2‰) higher in Δ_{47} than the $\Delta_{13C^{18}O^{16}O_2}$ value reactant carbonate. The range of results for these re-crystallized materials is greater than expected by analytical precision alone, suggesting either that our heating experiments failed to entirely equilibrate the starting materials at high

Table 4

Isotopic composition of carbon dioxide extracted from various carbonates before and after high-temperature recrystallization

Sample:	Before re-crystallization			After re-crystallization		
	Δ_{47}	$\delta^{13}C_{PDB}$	$\delta^{18}O_{SMOW}$	Δ_{47}	$\delta^{13}C_{PDB}$	$\delta^{18}O_{SMOW}$
47413 aragonite coral	0.74 ± 0.012	-6.51	41.43	0.28 ± 0.02	-7.82	40.21
MZ carbonate	0.64 ± 0.024	-13.15	35.18	0.22 ± 0.03	-13.82	34.74
Sigma carb	0.55 ± 0.025	-42.31	20.78	0.14 ± 0.03	-40.58	23.84

temperatures or that these samples experienced different degrees of re-equilibration during quenching. It is noteworthy that the Δ_{47} values of CO_2 extracted from these materials after re-crystallization is positively correlated with the Δ_{47} values of CO_2 extracted from them before re-crystallization (Table 4 and Fig. 4). This observation supports the interpretation that our heating protocol failed to fully equilibrate them during high-temperature re-crystallization (e.g., perhaps coarse grains retain a core that did not undergo re-crystallization and re-setting), and, by extension, that Reaction 1 is highly resistant to resetting in the absence of recrystallization. Therefore, the lowest Δ_{47} value measured in CO_2 released from re-crystallized Sigma-carb (0.14‰) likely represents the maximum fractionation accompanying acid digestion.

Despite these ambiguities, both the dependence of Δ_{47} of CO_2 on acid digestion temperature and the positive Δ_{47} values observed in CO_2 from high-temperature re-crystallized carbonate support the interpretation that acid digestion involves an isotopic fractionation of Δ_{47}, and that fractionation must be controlled if one is to achieve precise results for unknown samples (as one must do when analyzing $\delta^{18}O$ of carbonates by phosphoric acid digestion). Fortunately, in the case of Δ_{47} the temperature effect on the acid-digestion fractionation is subtle (0.0016‰ per °C), and so only need be controlled to within ± 10–15 °C to keep errors smaller than the standard errors of our most precise measurements. Further work will be needed to establish the exact amplitude of the acid digestion fractionation and whether or not the same fractionation applies to dolomites, magnesites, siderites and other non-$CaCO_3$ carbonates. For our present purposes, we restrict ourselves to analysis of calcite and aragonite at constant temperatures of acid digestion, and discuss variability in Δ_{47} of evolved CO_2 rather than attempting to correct such data back to inferred values of $\Delta_{^{13}C^{18}O^{16}O_2}$.

3.4. Calcite precipitated from aqueous solution at known, controlled temperatures

We examined the influence of carbonate growth temperature on the Δ_{47} value of CO_2 extracted from carbonate by analyzing CO_2 extracted from calcites grown in the laboratory at known, controlled temperatures from aqueous solutions (see Section 2.1, above, for a description of the methods used to synthesize these calcites). Table 5 summarizes the results of these analyses, and Figs. 4 and 5 plot the Δ_{47} values of CO_2 extracted from these calcites vs. $10^6/T^2$, where T is the measured growth temperature, in Kelvin. We also plot in Fig. 4 the value of $\Delta_{^{13}C^{18}O^{16}O_2}$ predicted by Schauble and Eiler (2004); for calcite that is in equilibrium with respect to Reaction 1, and the results of analyses of carbonates re-crystallized at 1100 °C. The data for calcites grown from aqueous solution show a correlation between the temperature of calcite precipitation and the Δ_{47} value carbon dioxide extracted from that calcite. A least-square

Table 5
Stable isotopic composition of synthetic calcites and natural aragonitic corals grown at known temperatures

Sample details	Growth temperature (°C)	$\delta^{18}O$ water SMOW	$\delta^{13}C_{PDB}$	$\delta^{18}O_{PDB}$	Δ_{47}
Calcite HA12	50 ± 2	−8.09	−21.53	−15.53	0.53
			−21.57	−15.61	0.60
			−21.58	−15.64	0.59
			−21.59	−15.64	0.54
			−21.59	−15.64	0.53
			−21.59	−15.65	0.58
			−21.59	−15.65	0.54
			−21.59	−15.64	0.55
Average			−21.58	−15.62	0.55
Standard error			0.021	0.040	0.011
Calcite HA3	1 ± 0.2	−7.6	−25.47	−5.21	0.77
			−25.47	−5.26	0.68
			−25.47	−5.26	0.80
			−25.47	−5.26	0.75
			−25.46	−5.26	0.71
			−25.47	−5.27	0.79
			−25.47	−5.25	0.72
			−25.47	−5.27	0.81
			−25.46	−5.27	0.81
			−25.47	−5.26	0.83
			−25.47	−5.28	0.85
Average			−25.47	−5.26	0.77
Standard error			0.004	0.019	0.016
Calcite HA9	33 ± 2	−7.37	−21.58	−11.34	0.65
			−21.59	−11.37	0.61
			−21.59	−11.38	0.61
			−21.59	−11.38	0.53
			−21.59	−11.37	0.63
			−21.59	−11.36	0.59
Average			−21.59	−11.37	0.60
Standard error			0.01	0.01	0.015
Calcite HA1	23 ± 1	−7.47	−17.52	−10.48	0.74
			−17.53	−10.50	0.55
			−17.53	−10.50	0.64
			−17.53	−10.49	0.70
			−17.53	−10.49	0.66
			−17.53	−10.49	0.62
Average			−17.53	−10.49	0.65
Standard error			0.01	0.01	0.025
Calcite HA2	23 ± 1	−7.54	−24.81	−10.30	0.70
			−24.82	−10.31	0.75
			−24.82	−10.31	0.73
			−24.82	−10.32	0.67
			−24.81	−10.30	0.71
Average			−24.81	−10.31	0.71
Standard error			0.005	0.008	0.014
Calcite HA7	23 ± 1	−7.88	−23.72	−11.16	0.58
			−23.75	−11.22	0.64
			−23.75	−11.22	0.55
			−23.75	−11.23	0.65
			−23.75	−11.22	0.69
Average			−23.74	−11.21	0.62
Standard error			0.01	0.03	0.025

(continued on next page)

Table 5 (continued)

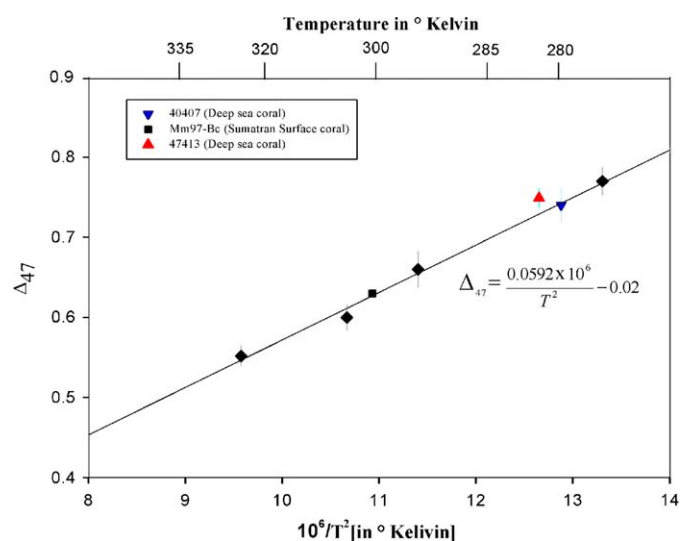| Sample details	Growth temperature (°C)	$\delta^{18}O$ water SMOW	$\delta^{13}C_{PDB}$	$\delta^{18}O_{PDB}$	Δ_{47}
Calcite HA4	50 ± 2	−7.45	−26.38	−14.67	0.52
			−26.38	−14.71	0.51
			−26.38	−14.71	0.56
			−26.38	−14.70	0.58
			−26.39	−14.70	0.61
			−26.38	−14.71	0.56
			−26.38	−14.70	0.52
Average			−26.38	−14.70	0.55
Standard error			0.004	0.015	0.014
Deep sea corals					
47407	5.5 ± 1.0	0.3 ± 0.2	−2.51	0.95	0.76
	(Adkins et al., 2003)		−2.51	0.95	0.70
			−2.51	0.94	0.75
Average			−2.51	0.95	0.74
Standard error			0.002	0.004	0.019
47413	8.0 ± 0.5	—	−6.52	−0.04	0.77
	(Adkins et al., 2003)		−6.51	−0.05	0.74
			−6.52	−0.05	0.74
			−6.52	−0.05	0.74
Average			−6.51	−0.05	0.74
Standard error			0.003	0.003	0.012
Surface coral Indonesian Surface Coral Mm97-Bc (~1960)	29.3 ± 2	—	−1.54	−5.27	0.63 ± 0.034

Fig. 5. Values of Δ_{47} of CO_2 extracted from calcites grown from aqueous solution (reproduced from Fig. 4) and of deep-sea and surface corals, plotted vs. $10^6/T^2$, where T is the known growth temperature in Kelvin. Note that both surface and deep-sea aragonitic corals generally conform to the trend defined by inorganic calcites. Deep-sea coral 47413 lies slightly (0.02‰) above this trend, perhaps suggesting a subtle 'vital effect' (this aliquot of this sample exhibits extreme vital effects on its $\delta^{13}C$ and $\delta^{18}O$ values; Table 5).

linear fit to these data yields the relationship (with correlation coefficient $r = 0.94$):

$$\Delta_{47} = 0.0592 \cdot 10^6 \cdot T^{-2} - 0.02.$$

Note that this equation relates the Δ_{47} value of carbon dioxide produced by phosphoric acid digestion of carbonate to the growth temperature of that carbonate. This is the simplest way to derive a paleotemperature equation directly from our data, but keep in mind that it reflects a combination of the temperature dependence of Reaction 1 and a ⩽ 0.14‰ enrichment in Δ_{47} relative to $\Delta_{13C^{18}O^{16}O_2}$ caused by acid digestion at 25 °C. Note also that this relationship might not be suitable for extrapolation to temperatures greater than 50 °C because we know from analysis of high-temperature re-crystallized calcites that the trend could pass through a Δ_{47} value as high as 0.14‰ when $10^6/T^2$ approaches 0. Nevertheless, this equation is suitable for interpolation and we suggest that it should be used for paleothermometry in the temperature range 1–50 °C until data become available for higher temperature experimental carbonates. The temperature sensitivity of this equation, combined with the best analytical precision for Δ_{47} that we have achieved on homogenized, high-purity calcite (ca. ±0.01‰), implies that Reaction 1 can be used to perform carbonate paleothermometry at near-earth-surface temperatures with precision of ca. ± 2 °C.

3.5. Analysis of natural corals grown at known, approximately constant temperatures

We find that our sample of *Porites* coral collected from the Sumatran surface ocean yields CO_2 having a Δ_{47} value of 0.63‰. When plotted in Fig. 5 at this coral's inferred growth temperature (29.3 ± 2 °C), this result is consistent with the temperature dependence we determined for synthetic calcite. Similarly, our analyses of two samples of the deep-sea coral, *D. dianthus*, yield Δ_{47} values of 0.74‰ (sample 47407, grown at 5 ± 1 °C) and 0.75‰ (sample 47413, grown at 8 ± 0.5 °C). These results are generally consistent with our inorganic calcite calibration (Fig. 5), although coral 47413 falls above that calibration by slightly more (0.02) than analytical uncertainty. All three of these corals are aragonitic, rich in organic matter, and, exhibit 'vital effects' in their $\delta^{18}O$ and $\delta^{13}C$ values (subtle in the case of Sumatran *Porites*; variable and severe in the case of deep-sea *D. dianthus*). The fact that all three samples yield results broadly consistent with our inorganic calcite calibration curve indicates several important things about the analysis of Δ_{47} values in natural carbonates:

- First, aragonite and calcite appear to exhibit the same relationship between carbonate growth temperature and the Δ_{47} value of CO_2 produced by phosphoric acid extraction.
- Second, vital effects that influence $\delta^{18}O$ and $\delta^{13}C$ of biologically mediated carbonate appear not to strongly influence Δ_{47} values of CO_2 extracted from that carbon-

ate. This is consistent with models for the vital effect, which assume that carbonate deposition occurs in local isotopic equilibrium (Bohm et al., 2000; Adkins et al., 2003). These models describe the vital effect by way of reservoir effects on the sampled C and O pools, not through kinetic fractionations. The equilibrium constant for Reaction 1 is independent of bulk isotopic composition, and so should not be sensitive to such reservoir effects. Note, however, that the aliquot of sample 47413 analyzed here has the greatest vital effect on its $\delta^{13}C$ and $\delta^{18}O$ values (Table 5; see also Adkins et al., 2003), and is the one sample to fall slightly above the inorganic calibration line. Thus, it is possible that vital effects produce a small increase in Δ_{47} relative to that predicted for inorganic calcite. Nevertheless, it is clear from Fig. 5 that this is a second-order perturbation on the general conformance of biogenic aragonite to our inorganic calcite calibration line.

- Finally, organic contaminants are potentially problematic for measurements of Δ_{47}, and so it is significant that these measurements yielded an easily interpreted result despite the large concentration of organic matter in the analyte corals. This result suggests that our CO_2 purification procedures are successful at removing whatever volatile organic contaminants might be produced by acid digestion of natural corals.

3.6. Speculations and initial evidence regarding the kinetics of ^{13}C–^{18}O 'clumping'

All geothermometers are meaningful only if one has a clear understanding of the geological environments in which they reach equilibrium and the effects of subsequent processes on re-setting that equilibrium. It seems likely to us, based on the known rapid kinetics of carbonate acid-base chemistry in aqueous solution (Zeebe et al., 1999) and previous experience with the kinetics of the carbonate–water oxygen isotope thermometer (Spero et al., 1997), that carbonate precipitation from water or re-crystallization in the presence of water often achieves or closely approaches local equilibrium with respect to Reaction 1 at any temperature $\geqslant 0$ °C (perhaps lower in the case of carbonates grown from brines or other low-temperature solutions). This inference is supported by our observation that carbonates grown in the temperature range 1–50 °C, both inorganically and biologically, are enriched in ^{13}C–^{18}O bonds by ca. 0.5–0.7‰, as expected by theory (Fig. 5). Note, however, that some processes, such as air–sea exchange and biological carbonate precipitation, can involve rapid, selective transport of dissolved inorganic carbon species, and consequential departures from local equilibrium with respect to oxygen isotope exchange reactions (Zeebe et al., 1999). We suspect such aqueous environments might also generate non-equilibrium abundances of ^{13}C–^{18}O bonds in dissolved inorganic carbon species, and thus in the carbonate minerals grown from such species.

The preservation of growth temperatures through later geological history raises a separate and more complicated set of questions: First, if carbonate grows at low temperature and is then heated without re-crystallization, at what temperatures and after what times will it re-equilibrate to take on the new, higher-temperature distribution? This question must be addressed before we can know how deeply buried a carbonate must be before it ceases to faithfully record its original precipitation temperature. Second, if a carbonate grows or re-crystallizes at high temperature and then cools, what will be the 'blocking temperature' at which Reaction 1 stops continuously re-equilibrating? This question must be answered before we can apply the ^{13}C–^{18}O carbonate thermometer to high-temperature metamorphic rocks.

These and related questions cannot be answered without studying the systematics of Δ_{47} measurements of CO_2 extracted from carbonates having high-temperature histories, and calibration of the ^{13}C–^{18}O order/disorder carbonate thermometer above 50 °C. Such work is beyond the scope of this study, although we can comment on several relevant observations found here. First, our attempts to re-crystallize calcite and aragonite at 1100 °C were only partially successful, based on the fact that differences in ^{13}C–^{18}O ordering among starting materials were not completely erased (Fig. 4 and Table 5). This suggests that Reaction 1 is surprisingly refractory to re-equilibration at high temperatures. Second, NBS-19 and MAR-J1 are calcites from Italian marbles that were metamorphosed to upper-greenschist facies during the mid-Tertiary and must have spent several (perhaps even tens of) million years in the shallow crust at temperatures below 200 °C (Molli et al., 2000). Carbon dioxide extracted from them has Δ_{47} values of 0.34–0.35‰. If the dashed curve linking our high- and low-temperature experimental data in Fig. 4 is correct, these values imply an apparent temperatures near ca. 200 °C. These data suggest that the 'blocking temperature' of the ^{13}C–^{18}O clumping reaction is significantly higher than earth-surface temperatures, even in rocks that have sat for millions of years at lower temperatures. These data are not yet sufficient for a quantitative analysis of the kinetics of Reaction 1, but point toward it being suitably refractory for preserving paleotemperatures over geological time scales, so long as re-crystallization has not occurred.

3.7. The seasonal cycle in ^{13}C–^{18}O ordering in Porites coral from the northern Red Sea

In this section, we discuss an application of the ^{13}C–^{18}O order/disorder carbonate paleothermometer to a recent *Porites* coral from the northern Red Sea. This thermometer has an ideal precision of ± 2 °C, 1σ, and the sample we examine is believed to have grown over only a ca. 6–10 °C temperature range (for reasons discussed below). Therefore, it should be possible for us to detect seasonality in growth temperature of this coral, but only if our methods can consistently generate data on natural materials

with precision of ± 0.01–$0.02\%_0$. This study is principally a test of the 'practical' limits to precision of our data. Serendipitously, these data also provide suggestive evidence for a vital effect or other artifact that produces a non-equilibrium ^{13}C–^{18}O ordering in at least some corals under some conditions (perhaps confirming our suggestion, above, regarding deep-sea coral 47413; see Fig. 5).

The northernmost Red Sea experiences unusually large seasonal variations in sea-surface temperature (SST) between winter minima averaging 21.2 °C and summer maxima averaging 27.6 °C (Rayner et al., 1996), but varying from place to place and year to year. Winter minima average 21.2 °C whereas summer maxima average 27.6 °C. Super-imposed on this seasonality is an inter-annual to decadal variability of ca. 1–2 °C. Note also that near-surface water temperatures in shallow coastal waters can experience local excursions outside the range observed by regional instrument records.

The Ras Muhammed Peninsula is surrounded by a narrow fringing shallow-water reef, including coral colonies growing at a water depth of ~5 m. Sample BRI-1 of *Porites lutea* was sampled in July, 1995 at Beacon rock (27°50.9′N, 34°18.6′E) located on the south side of the Ras Muhammed Peninsula, within the boundaries of Ras Muhammed National Park and near the southern tip of the Sinai Peninsula (Egypt). A core was collected from a hemispherical coral colony using an underwater pneumatic drill. The core was drilled vertically, parallel to the major axis of coral growth.

An X-ray radiograph of BRI-1 reveals density bands that we interpret as a seasonal growth pattern. We initially sampled this coral at 1-mm increments (measured perpendicular to the growth banding) using a low-speed drill. Splits of the drilled powders were reacted with phosphoric acid at 90 °C in a modified auto carbonate device and the purified CO_2 analyzed for $\delta^{13}C$ and $\delta^{18}O$ on a gas source stable isotope ratio mass spectrometer located at the stable isotope laboratory in Department of Earth and Planetary Sciences, Harvard University, Cambridge, Massachusetts. Additional splits of the same drilled powders were analyzed for Sr/Ca ratio by isotope dilution on an ICP-AES at Harvard. Both of these sets of measurements used techniques that have been previously described (Billups et al., 2004) and will be detailed further in a later publication. The results of these measurements are listed in Table 6 and plotted in Fig. 6. All three variables exhibit a seasonal cycle; maximum $\delta^{18}O$ values and Sr/Ca ratios and minimum $\delta^{13}C$ values correspond to cold winter temperatures (mid February) and the converses correspond to warmer summer temperatures. The strong seasonality in geochemical variables also corresponds to the density-banding pattern observed in the X-ray radiograph (low density corresponds to summer; high density corresponds to winter).

The arid climate in the northern Red Sea results in large and seasonally varying evaporative enrichments in the $\delta^{18}O$ of surface water, which prohibit straightforward application of the conventional carbonate–water oxygen isotope exchange thermometer to the $\delta^{18}O$ record in Fig. 6 (see Fel-

is et al., 2000). If we adopt Felis et al.'s (2000) empirical calibration of the $\delta^{18}O_{carbonate}$ thermometer in this region, we conclude that our sample (which varies in $\delta^{18}O_{PDB}$ from $-2.31\%_0$ to $-3.79\%_0$) grew at temperatures between 17.3 and 26.3 °C. Similarly, the Sr/Ca paleothermometer exhibits regional and genus-specific variations in its calibration that translate into errors of up to 4–6 °C if an inappropriate calibration is used (Marshall and McCulloch, 2002). However, Felis et al. (2004), present an empirical calibration for Red Sea corals that could be appropriate for our sample. If we apply this calibration to our record (which varies in Sr/Ca variation of from 9.08 and 9.62×10^{-3}), we find that it grew at temperatures between 28.5 and 19.5 °C. Both records imply summer temperature maxima of ca. 26–28 °C, similar to instrument records for the northern Red Sea (Genin et al., 1995), but winter minima of 17–20 °C, several degrees colder than the average for those records. These data suggest that Δ_{47} of CO_2 extracted from BRI-1 should vary by ca. $0.05\%_0$, between a summer minimum of ca. 0.63 and a winter maximum of ca. 0.68.

We re-sampled this coral core by cutting a slab parallel to the drilled transect shown in Fig. 7 and slowly rubbing it against an abrasive tool and recovering the powder this produced. This was done instead of drilling in order to minimize the possibility of disturbing the ^{13}C–^{18}O 'clumping' in carbonate by frictional heating. Our average sample spacing is 1–1.5 mm. The average growth rate of the coral varies between ~10 and 20 mm/year; the interval we sampled corresponds to a summer with two Sr/Ca minima (temperature maxima) separated by a brief, low-amplitude Sr/Ca maximum (at ~65 mm sampling distance), a broad, strong winter Sr/Ca maximum (temperature minimum) at ~75 mm, a broad, strong summer Sr/Ca minimum at ~85 mm, and a fall rise in Sr/Ca terminating at ~90 mm.

Recovered powders were reacted with phosphoric acid at 25 °C and their product CO_2 analyzed for $\delta^{13}C$, $\delta^{18}O$ and Δ_{47}, as for previous measurements described in this paper (Table 6). All extracted CO_2 samples were analyzed five times, so the expected, average external precision in Δ_{47} for each sample should be ca. ± 0.013. We assume that the acid digestion fractionation and the Δ_{47} temperature calibration for *Porites lutea* is the same as that for inorganic calcite (as appears to be true for Sumatran *Porites* coral and approximately true for deep-sea *D. dianthus* coral; Fig. 5). However, note that Red Sea corals have atypical calibrations of their Sr/Ca and $\delta^{18}O$ paleothermometers (Felis et al., 2000, 2004), and so we should perhaps be alert to the possibility of an unusual temperature sensitivity in the clumped isotope thermometer.

Table 5 lists the $\delta^{18}O$ and $\delta^{13}C$ of BRI-1 coral (corrected for acid fractionation) and the Δ_{47} value of CO_2 extracted from that same coral (not corrected for acid fractionation; i.e., these data can be directly compared with the experimental data in Figs. 4 and 5). The variations in $\delta^{18}O$ and $\delta^{13}C$ we observe are consistent with those previously analyzed on samples drilled from the same coral head (Fig. 6). Because the growth bands in this coral are curved
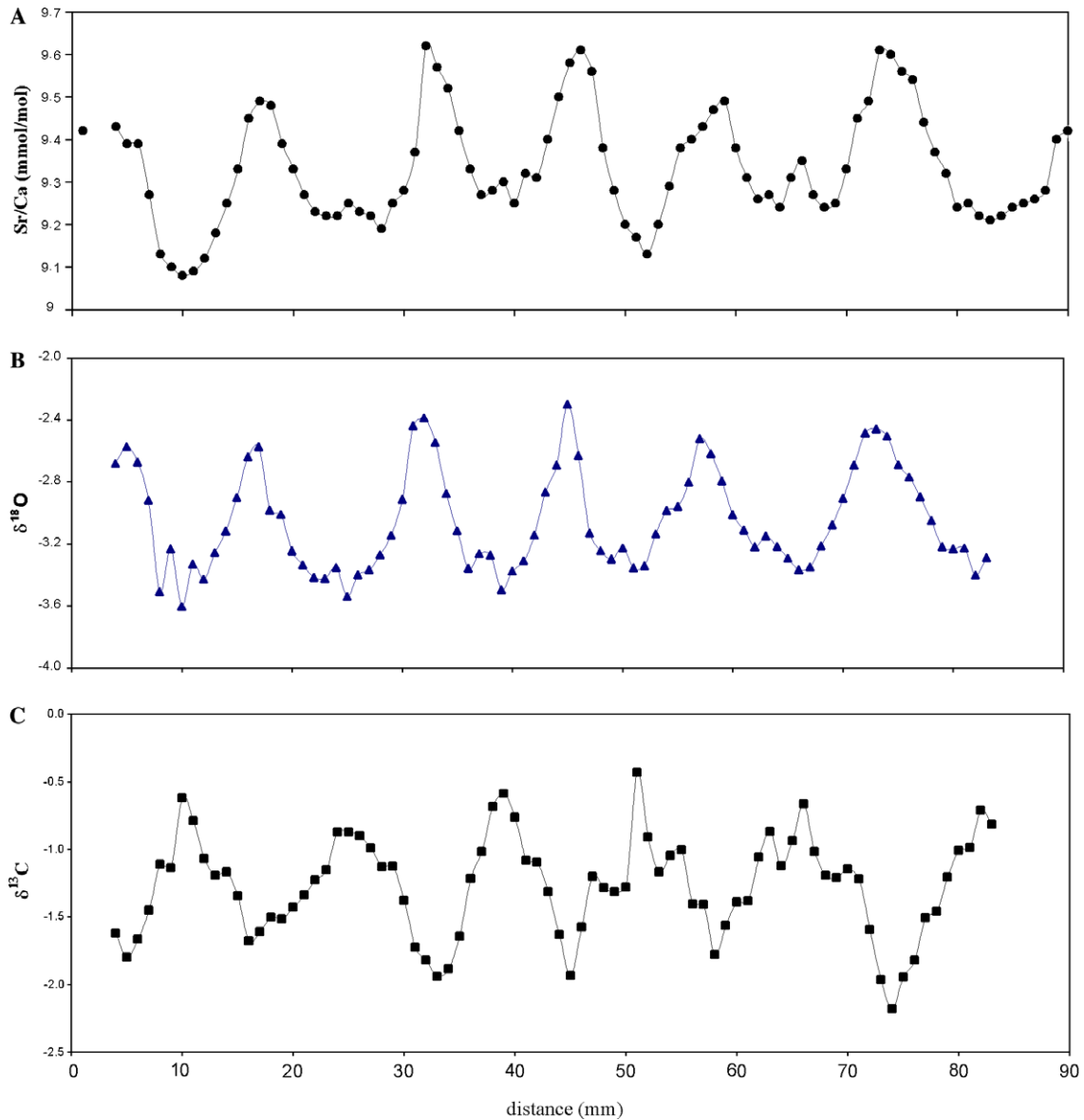
Fig. 6. Seasonal cycle in Sr/Ca ratio (A), $\delta^{13}C$ (B) and $\delta^{18}O$ (C) for 5 continuous annual bands from the Red Sea coral, of BRI-1. Maximum $\delta^{18}O$ values and Sr/Ca ratios and minimal $\delta^{13}C$ values correspond to cold winter temperatures and the converses correspond to warmer summer temperatures. The variations in Sr/Ca ratios between 9.08 and 9.62×10^{-3} correspond to a temperature range of between 28.5 and 19.5 °C, respectively, and variations in $\delta^{18}O$ between $-2.31\%_0$ to $-3.79\%_0$ correspond to a temperature range of between 17.3 and 26.3 (both based on the calibrations of Felis et al., 2000). The horizontal distance scale is the distance, in millimeters, from a point in the coral interior, and is measured perpendicular to growth banding visible to the naked eye.

and vary in thickness, we can only roughly correlate our samples with those previously analyzed for Sr/Ca. Our re-sampled interval lies closest to the band between 70 and 90 mm on the distance scale used in Fig. 6, but with an uncertainty on the order of several mm. Therefore, we used $\delta^{13}C$ values measured in both sets of samples (Figs. 6B and 7, inset) to correlate measurements of Δ_{47} in one sample suite with measurements of Sr/Ca ratio in the other.

Fig. 7 compares the Sr/Ca ratio and Δ_{47} stratigraphy, after spatially aligning the two data sets as described above. These Sr/Ca data are a sub-set of those shown in Fig. 6. Curves are fit through both data sets using an exponential smoothing technique (http://www.cas.lancs.ac.uk/

glossary_v1.1/tsd.html#smooth) contained within the SigmaPlot® software package (www.systat.com/products/ SigmaPlot/). Values of Δ_{47} exhibit spatial variations consistent with a quasi-sinusoidal curve having a period of $\sim$20 mm—similar to the seasonal cycles in Sr/Ca, $\delta^{18}O$ and $\delta^{13}C$. Thus, the first-order test we make in this section—attempting to retrieve a coherent seasonal cycle from a low-amplitude record—appears to have succeeded.

The Sr/Ca curve exhibits three minima over the interval sampled for Δ_{47}: one at $\sim$85, one at $\sim$68 mm and one at $\sim$62 mm. These latter two minima are separated by a low-amplitude maximum that likely reflects a summer or fall temperature anomaly rather than a winter. All of these
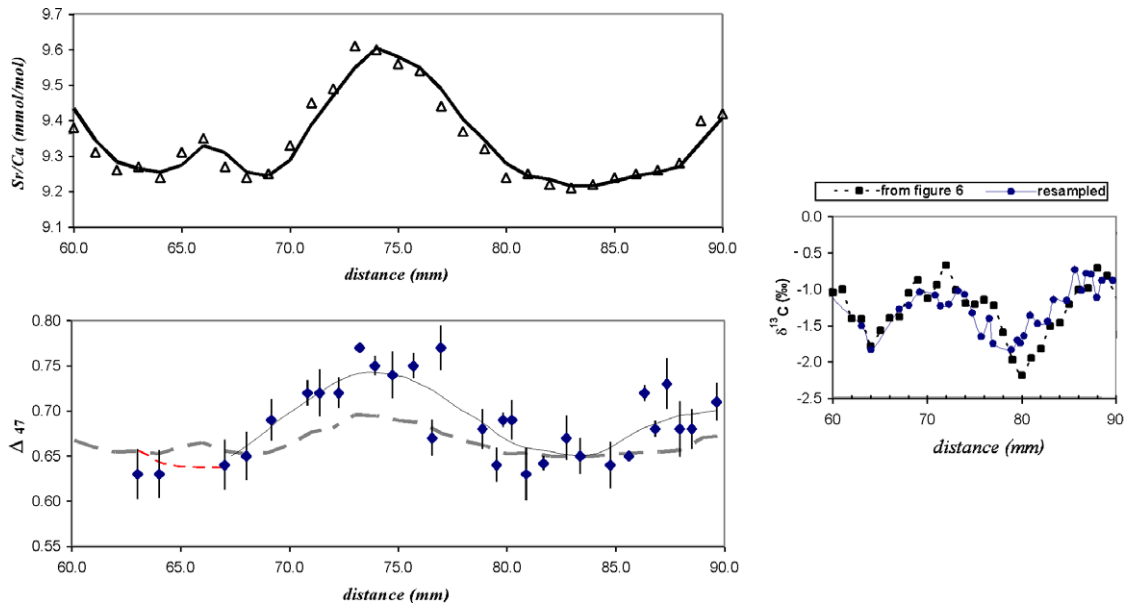
Fig. 7. (A) Reproduces the Sr/Ca ratio of BRI-1 coral from the last 30 mm of the traverse illustrated in Fig. 6. (B) Shows the Δ_{47} value of CO_2 extracted from aragonite recovered from a re-sampling of the same coral. The inset shows the goodness of fit between the two $\delta^{13}C$ data sets used to match the re-sampled Δ_{47} traverse with the original Sr/Ca traverse. The curves through both data sets in (A and B) are fit using a Gaussian smoothing technique and emphasize the seasonal cycle. The dashed curve in (B) indicates the Δ_{47} value predicted based on the Felis et al. (2000); calibration of the Sr/Ca record and the calibration of the Δ_{47} temperature sensitivity shown in Figs. 4 and 5. Values of Δ_{47} exhibit spatial variations consistent with a quasi-sinusoidal curve having a period of ~20 mm—similar to the seasonal cycles in Sr/Ca, $\delta^{18}O$ and $\delta^{13}C$. The maxima and minima in Sr/Ca and Δ_{47} line up with one another, as expected. However, the amplitude of Δ_{47} variations is greater than expected, perhaps reflecting a vital effect acting during winter growth in this coral.

minima correspond to minima in Δ_{47}. Similarly, both the winter maximum in Sr/Ca ratio at ~75 mm and the fall rise in Sr/Ca at ~90 correspond to two maxima in Δ_{47} (we did not measure the Δ_{47} value of carbonate corresponding to the low-amplitude maximum in Sr/Ca ratio at ~65 mm) (Fig. 7B). Thus, variations in Sr/Ca ratio and Δ_{47} value are in phase with one another and have the same sign, as expected if growth temperature controls both variables.

The three minima sampled by our traverse have average Δ_{47} values of between 0.64 and 0.65 (± 0.01), corresponding to apparent temperatures of between 26.5 and 24.5 (± 2) °C, respectively. These are consistent with summer maximum temperatures in the northern Red Sea, both as observed in instrument records and as inferred from interpretations of the $\delta^{18}O$ and Sr/Ca variations of Red Sea corals (Felis et al., 2000, 2004). Similarly, the late fall samples near 90 mm have an average Δ_{47} of 0.70 $\pm$ 0.02, corresponding to an apparent temperature of 15 $\pm$ 4. This average is lower than expected based on Sr/Ca and $\delta^{18}O$ records, but overlaps at the 1σ level the independently estimated winter temperature minimum. We have not bracketed this value with data for coral grown the following spring, so it is possible that we did not sample its maximum Δ_{47} value. Nevertheless, these data that do exist are consistent with the expected temperature variations. In these, respects, the carbonate clumped isotope thermometer appears to have successfully retrieved the known sea surface temperature history of the northern Red Sea, as recorded in BRI-1.

However, there is one noteworthy complication to our data set for BRI-1: The winter maximum Δ_{47} value ob-served near the sampling distance of 75 mm averages 0.74 $\pm$ 0.01, corresponding to an apparent temperature of 8 $\pm$ 2 °C—far lower than expected (Fig. 7B; expected Δ_{47} values are shown by a dashed curve). It seems unlikely to us that this discrepancy reflects analytical error because five closely spaced samples precisely define this high Δ_{47} value. It also seems unlikely that this discrepancy reflects true, lower-than expected winter temperatures at which BRI-1 grew, simply based on the weight of evidence from Sr/Ca and $\delta^{18}O$ thermometry (although both are based on empirical calibrations and might not have captured locally extreme temperatures experienced by the shallow-water sample we have studied). The only remaining possibility that occurs to us is that the temperature calibration for the carbonate clumped isotope thermometer in this sample of *Porites lutea* is more temperature sensitive than in inorganic calcite due to a vital effect. This is unexpected both because of the success of our application of the inorganic calibration to Sumatran *Porites* and deep-sea *D. dianthus* corals and because the inorganic calibration yielded acceptable temperatures for the summer, spring and fall parts of the BRI-1 record. Nevertheless, we hypothesize that the winter band in this sample grew under conditions that promoted an unknown vital effect and drove up the Δ_{47} value to values ca. 0.04 $\pm$ 0.01‰ higher than the thermodynamic equilibrium at its growth temperature. We speculate that this vital effect might be associated with slower than average growth during winter months, although there is insufficient information as yet to speculate on its physical cause. We ex-

Table 6
Results of Δ_{47} and Sr/Ca analyses of red sea coral (BRI-1) sample

Filed re-sampling				Drilled transect			
Sample No.	Distance (mm)	Δ_{47}	Standard error	Distance (mm)	Sr/Ca	$\delta^{13}C_{PDB}$	$\delta^{18}O_{PDB}$
A36	63.03	0.63	0.03	48	9.38	−1.29	−3.24
A35	64.03	0.63	0.03	49	9.28	−1.32	−3.30
A33	67.03	0.64	0.03	50	9.2	−1.28	−3.23
A32	68.03	0.65	0.03	51	9.17	−0.43	−3.35
A31	69.18	0.69	0.02	52	9.13	−0.91	−3.34
A29	70.84	0.72	0.01	53	9.2	−1.17	−3.13
A28	71.39	0.72	0.03	54	9.29	−1.05	−2.99
A27	72.27	0.72	0.02	55	9.38	−1.00	−2.96
A26	73.24	0.77	0.00	57	9.43	−1.41	−2.52
A25	73.94	0.75	0.01	58	9.47	−1.78	−2.62
A24	74.75	0.74	0.03	59	9.49	−1.57	−2.79
A23	75.71	0.75	0.01	60	9.38	−1.39	−3.01
A22	76.56	0.67	0.02	61	9.31	−1.38	−3.11
A21	76.97	0.77	0.03	62	9.26	−1.06	−3.22
A19	78.88	0.68	0.02	63	9.27	−0.87	−3.15
A18	79.53	0.64	0.02	64	9.24	−1.12	−3.22
A17	79.83	0.69	0.01	65	9.31	−0.94	−3.29
A16	80.23	0.69	0.02	66	9.35	−0.67	−3.37
A15	80.89	0.63	0.03	67	9.27	−1.02	−3.35
A14	81.68	0.64	0.01	68	9.24	−1.20	−3.21
A13	82.74	0.67	0.03	69	9.25	−1.21	−3.08
A12	83.38	0.65	0.02	70	9.33	−1.15	−2.91
A10	84.75	0.64	0.03	71	9.45	−1.22	−2.69
A9	85.61	0.65	0.00	72	9.49	−1.59	−2.48
A8	86.33	0.72	0.01	73	9.61	−1.97	−2.46
A7	86.82	0.68	0.01	74	9.6	−2.18	−2.50
A6	87.36	0.73	0.03	75	9.56	−1.95	−2.69
A5	87.95	0.68	0.03	76	9.54	−1.82	−2.77
A4	88.50	0.68	0.02	77	9.44	−1.51	−2.90
A2	89.64	0.71	0.02	78	9.37	−1.46	−3.05
				79	9.32	−1.21	−3.22
				80	9.24	−1.01	−3.23
				81	9.25	−0.99	−3.23
				82	9.22	−0.71	−3.40
				83	9.21	−0.81	−3.29
				84	9.22	−1.12	−3.20
				85	9.24	−1.12	−3.15
				86	9.25	−0.93	−3.11
				87	9.26	−1.30	−3.06
				88	9.28	−1.66	−2.78
				89	9.4	−2.05	−2.45

pect that a vital effect should lead to a correlation between Δ_{47} and $\delta^{13}C$, which is not observed. We suggest the most useful next step towards advancing these problems will be detailed study of cultured corals and other carbonate-precipitating organisms.

4. Summary and future directions

Ordering of ^{13}C and ^{18}O into bonds with each other within the crystal lattice of carbonate minerals is a temperature-dependent phenomenon that can be characterized by analysis of $^{13}C^{18}O^{16}O$ in CO_2 produced by phosphoric acid digestion. Phosphoric acid digestion appears to produce a small ($\leqslant 0.14‰$) enrichment in $^{13}C^{18}O^{16}O$ relative to proportions of $^{13}C^{18}O^{16}O_2^{2-}$ carbonate ions in reactant carbonate minerals, but this effect depends only weakly to acid reaction tem-

perature ($0.0016‰$ per °C) and so is relatively easily controlled.

Analyses of natural and synthetic carbonates grown at known temperatures demonstrate that 'clumping' of ^{13}C and ^{18}O isotopes in calcite and aragonite is subtle at earth-surface temperatures (ca. $0.7‰$ enrichments in $^{13}C-^{18}O$ bonds compared to their expected abundance in a material with randomly distributed stable isotopes). Moreover, the temperature dependence of this effect is subtle (the range is ca. $0.75–0.50‰$ between 1 and 50 °C, respectively). Nevertheless, proportions of $^{13}C-^{18}O$ bonds in carbonates can be measured consistently with external precision as good as $0.01–0.02‰$, even in complex natural materials, and so this thermometer can constrain growth temperature with precision as good as ± 2 °C. This uncertainty is too large for some problems (e.g., Pleistocene tropical SST variations, which are thought to be a few degrees or less) but sufficient for resolving many problems in paleoclimate research, meteoritics and the thermal history of soils and shallow crustal rocks.

The most important feature of the carbonate clumped isotope thermometer is that it is based on a homogeneous equilibrium, and thus it is rigorously defined based only on measurements of the isotopic content of carbonate minerals. That is, it is independent of the isotopic composition of water from which carbonate grew, or of any other phase with which carbonate might have co-existed. For this reason, it does not suffer from the 'ice volume problem' and analogous problems with carbonate–water exchange thermometers, which are rigorously defined only when the composition of carbonates and waters from which they grew are independently known. Also, the clumped isotope thermometer is based on a thermodynamic exchange equilibrium, and so is suitable for interpolation and applications to past times and diverse settings, unlike various empirical phylogenitic or morphological thermometers.

Analyses of biogenic aragonite from deep-sea and surface corals grown at known temperatures generally conform to the inorganic calibration of the carbonate clumped isotope thermometer; this includes samples of *D. dianthus* corals that exhibit pronounced 'vital effects' in their $\delta^{13}C$ and $\delta^{18}O$ values. Thus, there does not generally appear to be a 'vital' effect in biological materials. However, the *D. dianthus* specimen showing the greatest 'vital effect' releases CO_2 that is higher in Δ_{47} than expected by our inorganic calibration (by just more than analytical precision); similarly, seasonal variability in Δ_{47} in CO_2 from Red Sea *Porites* coral suggests winter growth may be associated with an anomalous enrichment in $^{13}C-^{18}O$ 'clumping'. We are unsure what physical processes might be responsible for such an effect, and suggest future studies of cultured organisms grown under controlled conditions will be required to fully understand it.

Analysis of carbonates that have undergone high-temperature re-crystallization followed by slow cooling suggests the blocking temperature of the carbonate clumped isotope thermometer (i.e., the temperature at which it ceas-

es to continuously re-equilibrate over geological timescales) is on the order of 200 °C. Thus, is seems likely that the sub-surface environments amenable to study by this approach will be those reached during diagenesis, catagenesis, burial metamorphism, anchimetamorphism, some types of ore formation, meteoritic aqueous alteration and similar environments in which water is abundant and temperatures are in the range 0–200 °C.

Data presented here calibrate the $^{13}C-^{18}O$ order/disorder carbonate thermometer for inorganic calcite between 1 and 50 °C, and document its applicability to biogenic aragonite. However, several additional studies are needed to fully flesh-out this thermometer's calibration. High-temperature experiments, perhaps using hydrothermal and/or piston-cylinder apparatus, are needed to define the temperature sensitivity of $^{13}C-^{18}O$ bond formation above 50 °C. Experiments on carbonates other than calcite and aragonite are needed at all temperatures; calibration data for dolomite will be particularly useful for studies of ancient carbonate sediments. Additional constraints on the kinetics of $^{13}C-^{18}O$ ordering during diagenesis, low-grade metamorphism and cooling of high-temperature rocks will be necessary before the carbonate clumped-isotope thermometer can be confidently applied to these important upper-crustal environments.

Acknowledgments

Associate editor: Miryam Bar-Matthews

References

Abram, N.J., Gagan, M.K., McCulloch, M.T., Chappell, J., Hantoro, W.S., 2003. Coral reef death during the 1997 Indian Ocean Dipole Linked to Indonesian Wildfires. *Science* **301**, 952–955.

Adkins, J.F., McIntyre, K., Schrag, D.P., 2002. The salinity, temperature, and delta O-18 of the glacial deep ocean. *Science* **298**, 1769–1773.

Adkins, J.F., Boyle, E.A., Curry, W.B., Lutringer, A., 2003. Stable isotopes in deep sea corals and a new mechanism for "vital effect". *Geochim. Cosmochim. Acta* **67**, 1129–1143.

Affek, H., Eiler, J., 2006. Abundance of mass 47 CO_2 in Urban air, car exhaust and human breath. *Geochim. Cosmochim. Acta.* **70**, 1–12.

Bigeleisen, J., Mayer, M.G., 1947. Calculation of equilibrium constants for isotopic exchange reactions. *J. Chem. Phys.* **15**, 261–267.

Billups, K., Rickaby, R.E.M., Schrag, D.P., 2004. Cenozoic pelagic Sr/Ca records: exploring a link to paleoproductivity. Paleocenography 19, Art. No. PA3005.

Bohm, F., Joachimski, M.M., Dullo, W.C., Eisenhauer, A., Lehnert, H., Reitner, J., Worheide, G., 2000. Oxygen isotope fractionation in marine aragonite of coralline sponges. *Geochim. Cosmochim. Acta* **64**, 1695–1703.

Dansgaard, W., Tauber, H., 1969. Glacier oxygen-18 content and Pleistocene ocean temperatures. *Science* **166**, 499.

Eiler, J.M., Schauble, E., 2004. $^{18}O^{13}C^{16}O$ in earth's atmosphere. *Geochim. Cosmochim. Acta* **68**, 4767–4777.

Emiliani, C., 1955. Pleistocene temperature. *J. Geol.* **63**, 538–578.

Emiliani, C., 1966a. Isotopic paleotemperature. *Science* **154**, 851–857.

Emiliani, C., 1966b. Paleotemperature analysis of Caribbean cores P6304-8 and P6304-9 and a generalized temperature curve for past 425000 Years. *J. Geol.* **74**, 109.

Epstein, S., Buchsbaum, R., Lowenstam, H., Urey, H.C., 1953. Revised carbonate water isotopic temperature scale. *Bull. Geol. Soc. Amer.* **64**, 1315–1326.

Felis, T., Patzold, J., Loya, Y., Fine, M., Nawar, A.H., Wefer, G., 2000. A coral oxygen isotope record from the Northern Red sea documenting NAO, ENSO, and North Pacific teleconnections on the Middle East climate variability since the year 1750. *Palaeoceanography* **15**, 679–694.

Felis, T., Lohmann, G., Kuhnert, H., Lorenz, S.J., Scholz, D., Patzold, J., Al-Rousan, S.A., Al-Moghrabi, S.M., 2004. Increased seasonality in Middle East temperatures during the last interglacial period. *Nature* **429**, 164–168.

Friedman, I., O'Neil, J.R., Cebula, G., 1982. Two new carbonate stable isotope standards. *Geostandard Newslett.* **6**, 11–12.

Genin, A., Lazar, B., Brenner, S., 1995. Vertical mixing and coral death in the Red Sea following the eruption of Mount Pinatubo. *Nature* **377**, 507–510.

Ghosh, P., Patecki, M., Rothe, M., Brand, W.A., 2005. Calcite-CO_2 mixed into CO_2 free air: a new CO_2-in-air stable isotope reference material for the VPDB Scale. *Rapid Commun. Mass Spectrom.* **19**, 1097–1119.

Kim, S.T., O'Neil, J.R., 1997. Equilibrium and non-equilibrium oxygen isotope effects in synthetic carbonates. *Geochim. Cosmochim. Acta* **61**, 3461–3475.

Leiss, B., Molli, G., 2003. High temperature texture in naturally deformed Carrara marble from the Alpi Apuane, Italy. *J. Struct. Geol.* **25**, 649–658.

Marshall, J.F., McCulloch, M.T., 2002. An assessment of the Sr/Ca ratio in shallow water hermatypic corals as a proxy for sea surface temperature. *Geochim. Cosmochim. Acta.* **66**, 3263–3280.

McCrea, J.M., 1950. On the isotopic chemistry of carbonates and a paleotemperature scale. *J. Chem. Phys.* **18**, 849–857.

Molli, G., Conti, P., Giorgetti, G., Meccheri, M., Oesterling, N., 2000. Microfabric study on the deformational and thermal history of the Alpi Aquane marble (Carrara marbles), Italy. *J. Struct. Geol.* **22**, 1809–1825.

Myers, E.R., Heine, V., Dove, M.T., 1998. Thermodynamics of Al/Al avoidance in the ordering of Al/Si tetrahedral framework structures. *Phys. Chem. Miner.* **25**, 457–464.

Natawidjaja, D.H., Sieh, K., Ward, S.N., Cheng, H., Edwards, R.L., Galetzka, J., Suwargadi, B.W., 2004. Paleogeodetic records of seismic and aseismic subduction from central Sumatran microatolls, Indonesia. *J. Geophys. Res.* **109**, B04306.

Natawidjaja, D.H., 2003. Neotectonics of the Sumatran Fault and paleogeodesy of the Sumatran subduction zone: Ph.D. thesis, Calif. Inst. of Technology; Pasadena.

O'Neil, J.R., Clayton, R.N., Mayeda, T.K., 1969. Oxygen isotope fractionation in divalent metal carbonates. *J. Chem. Phys.* **51**, 5547–5558.

Rayner, N.A., Horton, E.B., Parker, D.E., Folland, C.K., Hackett, R.B., 1996. Version 2.2 of the Global Sea Ice and Sea Surface Temperature Data Set, 1903–1994. Clim. Res. Tech. Note. 74, Hadley Centre, U.K. Meteorol. Off. Bracknell, England.

Schauble, E.A., Eiler, J.M., 2004. Theoretical estimates of equilibrium $^{13}C-^{18}O$ clumping in carbonates and organic acids [abstract]. *EOS, Trans. AGU.* **85** (47), Fall Meeting Supplement.

Shackleton, N.J., 1967. Oxygen isotope analyses and Pleistocene temper-atures re-assessed. *Nature* **215**, 5096.

Sharma, T., Clayton, R.N., 1965. Measurement of $^{18}O/^{16}O$ ratios of total oxygen of carbonates. *Geochim. Cosmochim. Acta* **29**, 1347–1353.

Schrag, D.P., Hampt, G., Murray, D.W., 1996. The temperature and oxygen isotopic composition of the glacial ocean. *Science* **272**, 1930–1932.

Schrag, D.P., Adkins, J.F., McIntyre, K., Alexander, J.L., Hodell, D.A., Charles, C.D., McManus, J.F., 2002. The oxygen isotopic composition of seawater during the Last Glacial Maximum. *Quaternary Sci. Rev.* **21**, 331.

Spero, H.J., Bijma, J., Lea, D.W., Bemis, B.E., 1997. Effect of seawater carbonate concentration on foraminiferal carbon and oxygen isotopes. *Nature* **390**, 497–500.

Swart, P.K., Burns, S.J., Leder, J.J., 1991. Fractionation of the stable isotopes of oxygen and carbon in carbon dioxide during the reaction of calcite with phosphoric acid as a function of temperature and technique. *Chem. Geol. (Isot. Geosci. Sec.)* **86**, 89–96.

Urey, H.C., 1947. The thermodynamic properties of isotopic substances. *J. Chem. Soc. London* **1947**, 561–581.

Wang, Z., Schauble, E.A., Eiler, J.M., 2004. Equilibrium thermodynamics of multiply substituted isotopologues of molecular gases. *Geochim. Cosmochim. Acta* **68**, 4779–4797.

Zeebe, R.E., Wolf-Gladrow, D.A., Jansen, H., 1999. On the time required to establish chemical and isotopic equilibrium in the carbon dioxide system in seawater. *Mar. Chem.* **65**, 135–153.